# SGN: Shifted Window-Based Hierarchical Variable Grouping for Multivariate Time Series Classification

Zenan Ying<sup>1</sup>, Jinke Wang<sup>1</sup>, Zhi Zheng<sup>1</sup>, Tong Xu<sup>1</sup>, Wei Chen<sup>1</sup>, Qi Liu<sup>1</sup>, Huijun Hou<sup>2</sup>

<sup>1</sup>State Key Laboratory of Cognitive Intelligence, University of Science and Technology of China <sup>2</sup>Nio

#### **Abstract**

Multivariate time series (MTS) classification has attracted increasing attention across various domains. Existing methods either decompose MTS into separate univariate series, ignoring inter-variable dependencies, or jointly model all variables, which may lead to over-smoothing and loss of semantic structure. These limitations become particularly pronounced when dealing with complex and heterogeneous variable types. To address these challenges, we propose SwinGroupNet (SGN), which explores a novel perspective for constructing variable interaction and temporal dependency. Specifically, SGN processes multi-scale time series using (1) Variable Group Embedding (VGE), which partitions variables into groups and performs independent group-wise embedding; (2) Multi-Scale Group Window Mixing (MGWM), which reconstructs variable interactions by modeling both intra-group and inter-group dependencies while extracting multi-scale temporal features; and (3) Periodic Window Shifting and Merging (PWSM), which exploits inherent periodic patterns to enable hierarchical temporal interaction and feature aggregation. Extensive experiments on diverse benchmark datasets from multiple domains demonstrate that SGN consistently achieves state-of-the-art performance, with an average improvement of 4.2% over existing methods. We release the source code at https://github.com/colison/SGN.

# 1 Introduction

Multivariate time series (MTS) consist of multiple temporal variables, each representing distinct dynamic patterns over time. MTS classification, which aims to analyze and model these temporal signals jointly to extract meaningful patterns for decision-making, has demonstrated significant importance across a wide range of application domains, including meteorology [1, 2], healthcare [3, 4, 5], industrial monitoring [6, 7], and human activity recognition [8, 9]. In recent years, many models have been developed specifically for temporal data analysis [10, 11, 12, 13, 14, 15, 16], achieving impressive performance across diverse applications. Among these, Convolutional Neural Networks (CNNs) have demonstrated continual development in the time series domain [17, 18, 19, 20] due to their strong ability to extract local features along the temporal dimension and have been shown to strike an effective balance between performance and computational efficiency [21].

In multivariate time series processing, in addition to modeling along the temporal dimension, capturing the dependencies among variables is equally critical. However, the complex and intertwined

<sup>\*</sup>Corresponding author.

dependencies among variables pose a significant challenge for effective modeling. Existing works have mainly adopted two strategies for modeling variable relationships, namely independent modeling and mixed modeling. Specifically, as shown in Figure 1(a), independent modeling-based methods [22, 23] treat multivariate data as a collection of univariate series and process each variable separately, thereby neglecting the inter-variable interdependencies. In contrast, as shown in Figure 1(b), mixed modeling-based methods [24, 25] jointly model all variables by mixing them together. However, when dealing with complex and heterogeneous variable types, this strategy blurs the semantic distinctions between variables [26], leading to excessive smoothing and making it difficult for the model to capture meaningful relationships [27].

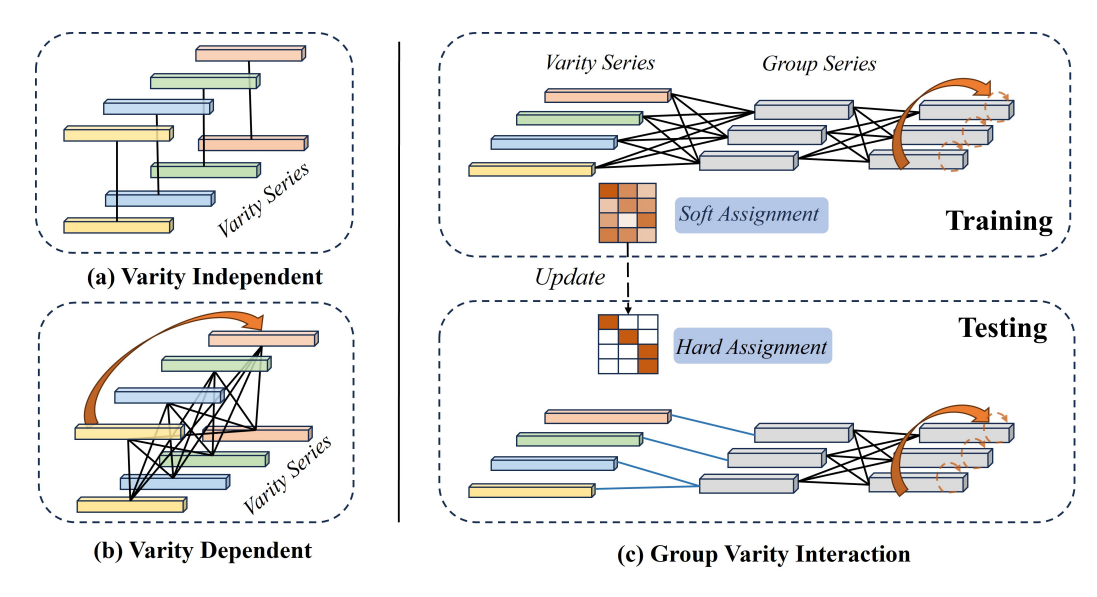


Figure 1: Illustration for Variety Interaction. (a) Variety Independent. (b) Variety Dependent. (c) Our Group Variety Interaction.

To address these challenges, in this paper, we introduce a novel perspective for modeling variable dependencies by transforming global variable interactions into structured intra-group and inter-group relationships. Specifically, we design the *Variable Group Embedding* (VGE) module, which partitions variables into groups based on an assignment matrix derived from their intrinsic similarity and performs independent group-wise embedding. As illustrated in Figure 1(c), the module employs soft assignments during training to allow flexible learning, and switches to hard assignments during inference to ensure stable group structures. This design is particularly effective when dealing with heterogeneous multivariate time series, as it enhances the model's capacity to capture diverse variable characteristics and their interactions.

Moreover, we segment the input sequence into small periodic windows and propose the *Multi-Scale Group Window Mixing* (MGWM) module, which reconstructs variable interactions by modeling both intra-group and inter-group dependencies while extracting temporal features at multiple scales. To further enhance the modeling of temporal dynamics, we introduce the *Periodic Window Shifting and Merging* (PWSM) module, which leverages inherent periodic patterns to enable hierarchical temporal interaction and feature aggregation. By integrating both variable and temporal perspectives, we present the **SwinGroupNet** (**SGN**) architecture, which performs structured variable grouping and interaction modeling in the variable dimension, and efficient multi-scale feature extraction in the temporal dimension. Meanwhile, SGN effectively balances performance and computational efficiency while capturing long-range dependencies and complex temporal patterns in multivariate time series. Extensive experiments on diverse datasets from various domains demonstrate that SGN consistently achieves state-of-the-art results. Our main contributions are summarized as follows:

• We propose a novel variable interaction strategy that transforms variable relationships into intra-group and inter-group dependencies based on variable grouping, unveiling underlying patterns and enhancing the interpretability of variable relationships.

- Extensive experiments demonstrate that SGN consistently outperforms existing state-of-theart methods, with an average accuracy gain of 4.2% and achieves near-perfect performance on several benchmarks, with accuracy approaching 100%.
- We exploit the inherent periodic characteristics of time series to enable hierarchical temporal feature extraction, allowing CNN-based models to capture long-term dependencies while maintaining high efficiency.

# 2 Related Work

#### 2.1 Convolution in Time Series Analysis

In recent years, convolutional methods have seen increasing adoption in time series analysis. CNN-based models typically focus on local patterns, with convolutional kernels adept at capturing localized features from the input. To expand the receptive field and capture long-range temporal dependencies, TCNs [28, 29] employ dilated convolutions. MICN [17] integrates both local and global features through multi-scale extraction, enabling the modeling of complex temporal patterns. TimesNet [18] transforms univariate time series into a two-dimensional format via periodic decomposition and applies 2D convolutions to capture intra-period and inter-period patterns. ModernTCN [19] further extends the receptive field by utilizing large convolutional kernels. TVNet [20] reshapes 1D sequences into 3D representations to extract hierarchical information across temporal dimensions. Despite these advancements, existing convolutional models often overlook the intricate dependencies between local and global contexts as well as heterogeneous variable interactions. Therefore, there remains considerable room for improvement in developing models that can comprehensively capture the complexity of multivariate time series.

#### 2.2 Variable Modeling Strategies in Multivariate Time Series

In multivariate time series analysis, variable modeling strategies aim to capture the dependencies among multiple variables. Given the inherently complex inter-variable relationships in such data, explicitly modeling these dependencies is crucial for learning comprehensive representations and enhancing model performance. Existing approaches can be broadly categorized into two strategies. Methods such as PatchTST [22], RLinear [16] treat each variable independently, enabling the model to specialize per variable. In contrast, models like iTransformer [24], Crossformer [25] mix all variables to learn cross-variable correlations, while CrossGNN [30] leverages graph structures to enhance the representation and understanding of variable interactions. These approaches have collectively advanced the field of multivariate time series analysis. Prior studies [31, 32, 33, 34] suggest that variable-independent models often offer greater model capacity, whereas variable-mixing strategies tend to exhibit improved robustness. However, striking a balance between these strategies remains a challenge. Recent work [35, 36, 37, 38]has explored the utility of variable clustering, yet in the time series domain, it remains unclear how best to translate variable-to-cluster relationships into meaningful interactions and how clustering can be leveraged to enhance inter-variable modeling. This remains an open and promising direction for further research.

#### 3 Method

As shown in Figure 2, we propose **SwinGroupNet** (**SGN**), a model for multivariate time series classification that captures structured interactions among variable groups. Specifically, we design a *Variable Group Embedding* (VGE) module that segments the input sequence into short periodic windows and embeds variables into groups based on their similarity. Next, the *Multi-Scale Group Window Mixing* (MGWM) module extracts features along both the temporal and variable dimensions. Furthermore, the *Periodic Window Shifting and Merging* (PWSM) module exploits inherent periodic patterns to enable hierarchical interaction and aggregation of temporal features. Finally, a projection layer produces the classification output. The following sections provide detailed descriptions of each component.

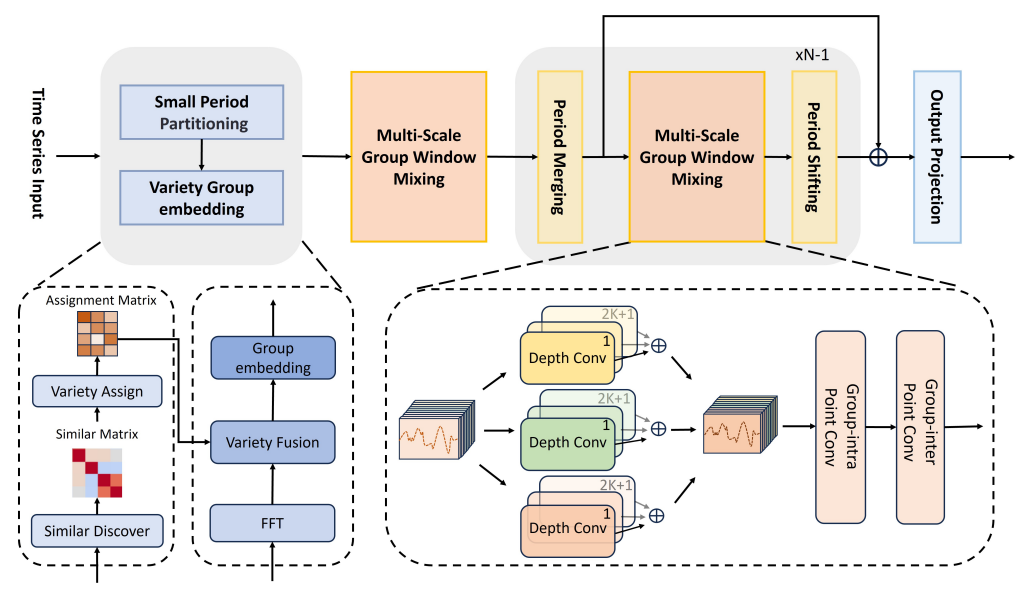


Figure 2: An illustration of the SwinGroupNet architecture.

#### 3.1 Variable Group Embedding

In this module, we first group the different variables of each sample and perform interactions within and across groups to capture the relationships among variables. For heterogeneous multivariate data, directly mixing all variables, including those with large differences, can cause over-smoothing and confuse the semantic meanings between variables. On the other hand, modeling each variable independently would neglect the dependencies among them. By clustering variables into groups, our method strikes a balance between these two extremes: it preserves the distinct properties of each variable while simultaneously mitigating interference among variables.

Specifically, for the input time series  $X \in \mathbb{R}^{C \times L}$ , where L represents the time length and C denotes the number of variables, the feature channels C are dynamically assigned to predefined groups G using the Gumbel-Softmax allocation mechanism [39, 40]. Given a categorical distribution, to avoid the collapse problem, instead of using randomly initialized unnormalized class logits, we compute the Brownian Distance Covariance (BDC) [41] between all variables. The specific formula is as follows:

$$dCov(X_1, X_2) = \sqrt{\frac{1}{n^2} \sum_{i,j=1}^n A'_{ij} B'_{ij}}.$$
(1)

Here,  $A'_{ij}$  and  $B'_{ij}$  denote the elements of the centered distance matrices for  $X_1$  and  $X_2$ , respectively, which are derived from the Euclidean distances between observations in  $X_1$  and  $X_2$ . Given the number of groups G, the similarity is then computed based on the BDC distance, and K-means clustering is applied to obtain G class logits vectors  $\Pi = [\pi_1, \pi_2, \ldots, \pi_G]$ , where each vector  $\pi_i \in \mathbb{R}^C$ . For more details, refer to Appendix A. And the Gumbel-Softmax sampling is defined as:

$$M_{ji} = \frac{\exp((\log \pi_{ij} + \epsilon_{ij})/\tau)}{\sum_{k=1}^{G} \exp((\log \pi_{kj} + \epsilon_{kj})/\tau)}, \quad j = 1, 2, \dots, C, \quad i = 1, 2, \dots, G.$$
 (2)

Here,  $\epsilon \sim \text{Gumbel}(0,1)$  denotes noise sampled from a standard Gumbel distribution, used to enhance the exploration during assignment. The parameter  $\tau > 0$  is the temperature that controls the smoothness of the resulting distribution. It is gradually annealed following an exponential decay schedule during training.

The input tensor X is grouped according to the assignment matrix  $M \in \mathbb{R}^{C \times G}$ , where  $M_{ji}$  denotes the soft assignment probability of variable j to group i. We use Softmax-based soft assignment

during training and one-hot hard assignment during evaluation. To avoid inconsistent assignments and unstable optimization, we introduce a variable similarity regularization term to guide the Gumbel-based assignment towards more reasonable groupings. During the training process, the cosine similarity  $S_{ij}$  is dynamically computed with Variety  $X_i$  and  $X_j$  after normalizing the variables to obtain the similarity matrix  $S \in \mathbb{R}^{C \times C}$ , while incorporating the assignment matrix into the loss function. The specific regularization loss formula is as follows:

$$\mathcal{L}_{\text{sim}} = \sum_{i,j} S_{ij} \cdot ||M_i - M_j||^2.$$
 (3)

Therefore, the final loss is given by  $\mathcal{L} = \mathcal{L}_{task} + \beta \mathcal{L}_{sim}$  and  $\beta$  is a regularization parameter for balancing classification accuracy and cluster quality. Meanwhile, to facilitate effective intra-group and inter-group interactions after variable grouping, we perform independent embeddings for each variable group.

# 3.2 Multi-Scale Group Window Mixing

**Small Periodic Window Partitioning.** Specifically, periodic patterns in time series often rely on information in the frequency domain. To capture this, we first apply the Fast Fourier Transform (FFT) to the input data X and compute the mean of the amplitude spectrum [18].

$$A = Avg(Amp(FFT(X))). (4)$$

To achieve a better trade-off between performance and efficiency, instead of selecting the top-K periods with the highest amplitudes, we choose the smallest period among the top-K candidates as the cycle window.

$$P = \min \left\{ \frac{L}{f_i} \mid f_i \in \operatorname{argTopK}(A), \ i = 1, 2, \dots, K \right\}. \tag{5}$$

Each  $\frac{L}{f_i}$  corresponds to the i-th dominant frequency component. Given the selected period window P, we divide the time series into  $N = \lceil \frac{L}{P} \rceil$  segments, where zero-padding is applied at the end if L is not divisible by P, obtain the output sequence as  $X \in \mathbb{R}^{C \times N \times P}$ . Considering the extensibility of periodic patterns, we further incorporate multiple scales by merging additional period windows corresponding to the remaining Top-K dominant frequencies. This approach allows us to extract multi-scale periodic information and enhance computational efficiency.

Multi-Scale Group Window Extracting. Given a multivariate time series  $X \in \mathbb{R}^{C \times N \times P}$ , to better extract temporal and variable features, We follow the design proposed by Liu [42, 43], adopting a combination of depthwise convolution and pointwise convolution to separate temporal and variable information. Along the temporal dimension, we apply multiple convolution kernels of different receptive fields within each period window to perform multi-scale feature extraction like [18, 44, 45]. The extracted features from different scales are then aggregated through average pooling to enhance the robustness of the output representations. The detailed formulation is given as follows:

$$Y = \frac{1}{K} \sum_{i=0}^{K-1} \mathcal{C}_g^{(k_i)}(X), \quad k_i = 2i+1, \quad \forall i \in \{0, 1, \dots, K-1\},$$
 (6)

where  $\mathcal{C}_g^{(k_i)}(\cdot)$  denotes a grouped convolution operation applied at a specific scale parameterized by the kernel size  $k_i$ . Across the variable dimension, we decouple the full variable interactions into intra-group and inter-group interactions, effectively mitigating the oversmoothing issue commonly observed in deep architectures. Specifically, we apply separate pointwise convolutions within each group and across different groups, respectively, to jointly learn fine-grained dependencies among variables within a group and higher-order relationships among different groups. The detailed structure of the Multi Swin Window block is illustrated in Figure 2.

## 3.3 Periodic Window Shifting and Merging

**Periodic Window Shifting**. Although the above procedure successfully extracts features from small periodic windows, it lacks connections across different windows, which limits interactions across periodic segments. Inspired by the Swin Transformer [46], we leverage the phase shift property of periodic signals to enable efficient cross-window communication. Specifically, we first perform a cyclic left shift of the input time series X by P/2 units, where P is the periodic window length. We then redivide the shifted sequence into windows and extract the features accordingly. The process can be formulated as follows:

$$X_{\text{shifted}} = \mathcal{T}_{-\frac{P}{2}} \left( \text{Reshape}(X, (C, N \cdot P)) \right), \tag{7}$$

where  $\mathcal{T}_{-\frac{P}{2}}$  denotes a cyclic left shift operation by P/2 units. After feature extraction, we apply a cyclic right shift to restore the original temporal order. This operation introduces cross-window interactions while maintaining computational efficiency. By alternating between standard window partitioning and shifted partitioning, the model captures both intra-window and inter-window dependencies within the same periodic scale. Specifically, as shown in Figure 3, this approach effectively enhances the model's ability to capture complex temporal patterns.

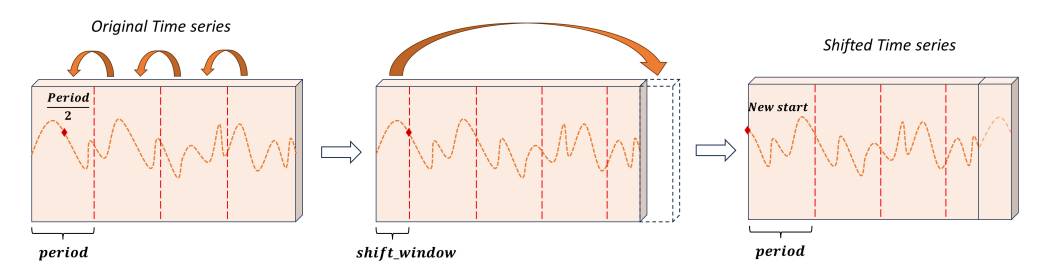


Figure 3: Illustration of Periodic Window Shifting Block.

**Periodic Window Merging.** Based on the extensibility of periodic patterns, we further merge adjacent periodic windows to capture features over extended cycles. Specifically, two neighboring periodic segments are combined to generate representations corresponding to 2P-length cycles. Notably, such extended periods often correspond to dominant frequencies among the top-k spectral components. To enhance computational efficiency, we employ an adaptive merging strategy based on the number of detected periodic windows. When the number of periods exceeds four, we adopt an exponentially decaying merging scheme, in which non-overlapping adjacent windows are progressively merged. In contrast, when fewer than four periods are present, we switch to a linearly decaying merging strategy that allows overlapping windows, thereby enabling more effective feature extraction from larger periodic structures.

# 4 Experiments

**Dataset.** To evaluate the effectiveness of the proposed SwinGroupNet model, we conduct extensive experiments on a diverse set of multivariate time series datasets. The detailed main dataset information is provided in Table 1. Furthermore, to comprehensively assess the generalization ability of our model, we additionally select 10 multivariate datasets from the UEA Time Series Classification Archive, which was introduced by Bagnall [47]. For additional details on data characteristics and preprocessing, please refer to Appendix B.

**Baseline.** We include 10 state-of-the-art time series methods as baselines to comprehensively evaluate the performance of our proposed method. These methods include six Transformer-based models: Reformer [48], iTransformer [24], Crossformer [25], FEDformer [14], PatchTST [22], Medformer [49]; One MLP-based model: DLinear [15]; And three CNN-based models: MICN [17], TimesNet [18], ModernTCN [19].

**Implementation.** In the main datasets, we adopt six evaluation metrics: Accuracy, Precision, Recall, F1 Score, AUROC, and AUPRC. The training process is conducted using five different random seeds

Table 1: Summary of the four benchmark datasets used in our experiments. The table lists the number of samples, classes, channels, length, sampling rate and modality.

Datasets	Samples	Timestamps	Channel	Class	Sampling Rate	Modality	FileSize
TDBRAIN	6,240	256	33	2	256 Hz	EEG	571MB
PTB-XL	191,400	250	12	5	250 Hz	ECG	4.28GB
FLAAP	13,123	100	6	10	100 Hz	HAR	60MB
UCI-HAR	10,299	128	9	6	50 Hz	HAR	91MB

(41–45) on fixed training, validation, and test splits to compute the mean and standard deviation of the results. For the 10 multivariate datasets from the UEA Time Series Classification Archive, we follow the standard preprocessing protocol established by Wu [18]. See Appendix C.1 for more implementation details.

Table 2: Performance comparison on Main Datasets from different domains. **Bold** values represent the best performance, and <u>underlined</u> values indicate the second-best scores.

Dataset	Model	Accuracy	Precision	Recall	F1 Score	AUROC	AUPRC
	Reformer	$87.92 \pm 2.01$	$88.64 \pm 1.40$	$87.92 \pm 2.01$	$87.85 \pm 2.08$	$96.30 \pm 0.54$	$96.40 \pm 0.45$
	Crossformer	$81.56 \pm 2.19$	$81.97 \pm 2.25$	$81.56 \pm 2.19$	$81.50 \pm 2.20$	$91.20 \pm 1.78$	$91.51 \pm 1.71$
	FEDformer	$78.13 \pm 1.98$	$78.52 \pm 1.91$	$78.13 \pm 1.98$	$78.04 \pm 2.01$	$86.56 \pm 1.86$	$86.48 \pm 1.99$
	iTransformer	$74.67 \pm 1.06$	$74.71 \pm 1.06$	$74.67 \pm 1.06$	$74.65 \pm 1.06$	$83.37 \pm 1.14$	$83.73 \pm 1.27$
	PatchTST	$79.25 \pm 3.79$	$79.60 \pm 4.09$	$79.25 \pm 3.79$	$79.20 \pm 3.77$	$87.95 \pm 4.96$	$86.36 \pm 6.67$
TDBRAIN	Medformer	$89.62 \pm 0.81$	$89.68 \pm 0.78$	$89.62 \pm 0.81$	$89.62 \pm 0.81$	$96.41 \pm 0.35$	$96.51 \pm 0.33$
	Dlinear	$54.73 \pm 2.14$	$54.79 \pm 2.48$	$54.73 \pm 2.14$	$54.62 \pm 2.13$	$55.83 \pm 2.36$	$54.73 \pm 1.98$
	Timesnet	$95.08 \pm 0.56$	$95.11 \pm 0.58$	$95.08 \pm 0.56$	$95.08 \pm 0.56$	$98.92 \pm 0.19$	$98.95 \pm 0.19$
	MICN	$90.92 \pm 2.24$	$\overline{91.37 \pm 1.82}$	$90.92 \pm 2.44$	$90.89 \pm 2.46$	$97.58 \pm 1.84$	$97.62 \pm 1.93$
	ModernTCN	$87.60 \pm 2.03$	$88.10 \pm 1.38$	$87.60 \pm 2.03$	$87.54 \pm 2.13$	$95.72 \pm 0.87$	$95.87 \pm 0.94$
	SGN (Ours)	$99.90 \pm 0.10$	$99.89 \pm 0.11$	$99.90 \pm 0.10$	$99.90 \pm 0.10$	$100.00 \pm 0.00$	$100.00\pm0.00$
	Reformer	$71.72 \pm 0.43$	$63.12 \pm 1.02$	$59.20 \pm 0.75$	$60.69 \pm 0.18$	$88.80 \pm 0.24$	$64.72 \pm 0.47$
	Crossformer	$73.30 \pm 0.14$	$65.06 \pm 0.35$	$61.23 \pm 0.33$	$62.59 \pm 0.14$	$90.02 \pm 0.06$	$67.43 \pm 0.22$
	FEDformer	$\overline{57.20 \pm 9.47}$	$52.38 \pm 6.09$	$49.04 \pm 7.26$	$47.89 \pm 8.44$	$82.13 \pm 4.17$	$\overline{52.31 \pm 7.03}$
	iTransformer	$69.28 \pm 0.22$	$59.59 \pm 0.45$	$54.62 \pm 0.18$	$56.20 \pm 0.19$	$86.71 \pm 0.10$	$60.27 \pm 0.21$
	PatchTST	$73.23 \pm 0.25$	$65.70 \pm 0.64$	$60.82 \pm 0.76$	$62.61 \pm 0.34$	$89.74 \pm 0.19$	$67.32 \pm 0.22$
PTB-XL	Medformer	$72.87 \pm 0.23$	$\overline{64.14 \pm 0.42}$	$60.60 \pm 0.46$	$62.02 \pm 0.37$	$89.66 \pm 0.13$	$66.39 \pm 0.22$
	Dlinear	$45.49 \pm 0.03$	$20.25 \pm 9.92$	$20.10 \pm 0.09$	$12.78 \pm 0.26$	$50.63 \pm 0.12$	$20.75 \pm 0.13$
	Timesnet	$71.80 \pm 0.53$	$62.73 \pm 0.88$	$59.53 \pm 0.99$	$60.72 \pm 0.49$	$88.27 \pm 0.65$	$63.53 \pm 1.07$
	MICN	$67.33 \pm 0.36$	$56.98 \pm 0.93$	$51.90 \pm 0.81$	$53.29 \pm 0.52$	$85.63 \pm 0.29$	$57.70 \pm 0.49$
	ModernTCN	$72.85 \pm 0.19$	$63.68 \pm 0.43$	$60.20 \pm 0.82$	$61.33 \pm 0.64$	$89.54 \pm 0.31$	$66.00 \pm 0.46$
	SGN (Ours)	$73.80 \pm 0.34$	$65.88 \pm 0.47$	$62.17 \pm 0.61$	$63.43 \pm 0.49$	$90.25 \pm 0.17$	$67.76 \pm 0.58$
	Reformer	$70.88 \pm 0.88$	$71.47 \pm 0.77$	$70.22 \pm 1.13$	$70.19 \pm 1.02$	$95.27 \pm 0.28$	$74.64 \pm 1.24$
	Crossformer	$76.33 \pm 0.81$	$76.25 \pm 0.93$	$76.15 \pm 0.84$	$76.14 \pm 0.88$	$96.93 \pm 0.13$	$80.25 \pm 0.69$
	FEDformer	$68.30 \pm 2.06$	$\overline{69.18 \pm 0.96}$	$67.60 \pm 2.12$	$\overline{66.80 \pm 2.96}$	$94.15 \pm 0.76$	$70.85 \pm 3.12$
	iTransformer	$75.83 \pm 0.49$	$75.70 \pm 0.65$	$75.82 \pm 0.56$	$75.57 \pm 0.53$	$96.70 \pm 0.14$	$80.32 \pm 0.64$
	PatchTST	$56.23 \pm 0.28$	$56.21 \pm 0.69$	$55.45 \pm 0.24$	$55.57 \pm 0.35$	$88.92 \pm 0.09$	$58.40 \pm 0.28$
FLAAP	Medformer	$74.00 \pm 2.37$	$74.53 \pm 2.48$	$73.84 \pm 2.61$	$73.57 \pm 2.55$	$96.58 \pm 0.60$	$78.91 \pm 2.90$
	Dlinear	$30.26 \pm 1.46$	$27.46 \pm 1.06$	$28.20 \pm 0.99$	$25.71 \pm 0.49$	$70.76 \pm 0.49$	$26.70 \pm 0.23$
	Timesnet	$73.79 \pm 0.94$	$73.55 \pm 0.78$	$73.57 \pm 0.92$	$72.82 \pm 0.96$	$95.70 \pm 0.12$	$77.30 \pm 0.84$
	MICN	$52.63 \pm 0.59$	$51.74 \pm 0.76$	$51.45 \pm 0.50$	$50.84 \pm 0.56$	$88.35 \pm 0.32$	$48.81 \pm 0.45$
	ModernTCN	$71.66 \pm 1.69$	$72.23 \pm 1.45$	$71.55 \pm 1.66$	$71.37 \pm 1.46$	$95.04 \pm 0.30$	$73.47 \pm 1.99$
	SGN (Ours)	$80.81 \pm 0.41$	$80.68 \pm 0.32$	$80.35 \pm 0.50$	$80.35 \pm 0.41$	$97.42 \pm 0.10$	$85.73 \pm 0.37$
	Reformer	$90.00 \pm 0.63$	$90.10 \pm 0.71$	$90.14 \pm 0.75$	$89.92 \pm 0.63$	$98.97 \pm 0.08$	$95.86 \pm 0.29$
	Crossformer	$90.66 \pm 1.02$	$90.83 \pm 0.98$	$90.69 \pm 1.02$	$90.68 \pm 1.04$	$99.14 \pm 0.15$	$96.08 \pm 0.61$
	FEDformer	$86.90 \pm 3.46$	$88.57 \pm 0.99$	$87.58 \pm 3.15$	$87.71 \pm 2.24$	$97.66 \pm 1.08$	$92.87 \pm 1.64$
	iTransformer	$93.47 \pm 0.15$	$93.59 \pm 0.23$	$93.49 \pm 0.14$	$93.46 \pm 0.16$	$99.53 \pm 0.02$	$97.91 \pm 0.01$
	PatchTST	$86.83 \pm 0.68$	$87.59 \pm 0.68$	$87.15 \pm 0.78$	$87.17 \pm 0.77$	$98.43 \pm 0.12$	$93.57 \pm 0.50$
UCI-HAR	Medformer	$90.17 \pm 0.52$	$90.36 \pm 0.66$	$90.30 \pm 0.68$	$90.27 \pm 0.66$	$99.10 \pm 0.07$	$95.84 \pm 0.75$
	Dlinear	$61.28 \pm 1.26$	$60.89 \pm 1.34$	$59.37 \pm 1.36$	$58.83 \pm 1.00$	$84.70 \pm 0.35$	$59.29 \pm 0.41$
	Timesnet	$92.71 \pm 0.50$	$92.78 \pm 0.46$	$92.86 \pm 0.53$	$92.75 \pm 0.51$	$99.25 \pm 0.04$	$96.87 \pm 0.24$
	MICN	$86.23 \pm 0.73$	$86.72 \pm 0.66$	$86.26 \pm 0.73$	$86.22 \pm 0.73$	$98.63 \pm 0.15$	$92.94 \pm 1.19$
	ModernTCN	$92.75 \pm 2.03$	$92.96 \pm 2.31$	$92.88 \pm 2.16$	$92.80 \pm 2.18$	$99.35 \pm 0.19$	$96.98 \pm 0.91$
	SGN (Ours)	$95.62 \pm 0.72$	$95.79 \pm 0.69$	$95.61 \pm 0.72$	$95.64 \pm 0.70$	$99.77 \pm 0.08$	$98.96 \pm 0.39$

# 4.1 Result of Main Datasets

**Setups.** In our main experimental setup, the training, validation, and testing sets are partitioned either by subject or according to a fixed ratio, depending on the dataset characteristics. Samples from each subject are assigned to the respective sets following a fixed allocation ratio. Importantly, samples

from the same subject are restricted to a single subset to avoid any data leakage. This design ensures the independence and objectivity of model training and evaluation.

Results. As shown in Table 2, SGN consistently outperforms ten strong baseline models across four benchmark datasets of different types, achieving the best performance on all evaluation metrics. On average, in terms of accuracy, our method surpasses the second-best approach 4.2%. Specifically, SGN yields significant improvements on TDBRAIN, FLAPP, and UCI-HAR, outperforming the second-best models by 4.8%, 4.5%, and 2.2%, highlighting the advantage of modeling variable dependencies through variable grouping. Notably, on the TDBRAIN dataset, SGN achieves an impressive approaching 100% accuracy. However, the performance gain on the PTB-XL dataset is relatively marginal. This can be attributed to the inherent variable similarity structure: TDBRAIN exhibits clear boundaries among variable clusters, enabling effective group-based modeling, while PTB-XL presents high similarity across variables with blurred boundaries, causing most variables to be grouped together. As a result, group interactions degenerate into a conventional mixed-variable approach. The variable similarity visualizations for each dataset are provided in Appendix B.6.

Dataset / Model	W.+MUSE	MFCN	TapNet	ShapeNet	TodyNet	SVPT	ShapeFormer	MPTSNet	SGN (Ours)
Articulary Word Recognition	99.0	97.3	98.7	98.7	98.7	99.3	99.0	97.7	99.0
AtrialFibrillation	33.3	26.7	33.3	40.0	46.7	40.0	53.3	53.3	66.7
BasicMotions	100.0	95.0	100.0	100.0	100.0	100.0	100.0	100.0	100.0
Cricket	100.0	91.7	95.8	98.6	100.0	100.0	94.4	94.4	100.0
DuckDuckGeese	57.5	67.5	57.5	72.5	58.0	70.0	64.0	68.0	64.0
Epilepsy	100.0	76.1	97.1	98.7	97.1	98.6	98.6	97.1	97.8
EthanolConcentration	13.3	37.3	32.3	31.2	35.0	33.1	41.1	43.3	44.5
ERing	43.0	13.3	13.3	13.3	91.5	93.7	87.4	94.4	95.9
FaceDetection	54.5	54.5	55.6	60.2	62.7	51.2	65.8	69.8	70.3
FingerMovements	49.0	58.0	53.0	58.9	67.6	60.0	55.0	64.0	64.0
HandMovementDirection	36.5	36.5	37.8	33.8	64.9	39.2	41.9	63.5	75.7
Handwriting	60.5	28.6	35.7	45.1	43.6	43.3	30.2	34.4	50.4
Heartbeat	72.7	66.3	75.1	75.6	75.6	79.0	81.5	75.6	77.1
Libras	87.8	85.6	85.0	85.6	85.0	88.3	95.5	87.2	83.9
LSST	59.0	37.3	56.8	59.0	61.5	66.6	63.8	60.4	63.7
MotorImagery	50.0	51.0	59.0	61.0	64.0	65.0	N/A	65.0	65.0
NATOPS	87.0	88.9	93.9	88.3	97.2	90.6	96.1	94.4	98.3
PenDigits	94.8	97.8	98.0	97.7	98.7	98.3	99.1	98.9	99.1
PEMS-SF	N/A	69.9	75.1	75.1	78.0	86.7	N/A	94.2	88.4
PhonemeSpectra	19.0	11.0	17.5	29.8	30.9	17.6	29.3	14.4	23.1
RacketSports	93.4	80.3	86.8	88.2	80.3	84.2	88.8	87.5	93.4
SelfRegulationSCP1	71.0	87.4	65.2	78.2	89.8	88.4	91.8	92.8	93.9
SelfRegulationSCP2	46.0	47.2	55.0	57.8	55.0	60.0	56.1	57.2	60.6
StandWalkJump	33.3	6.7	40.0	53.3	46.7	46.7	66.7	53.3	53.3
UWaveGestureLibrary	91.6	89.1	89.4	90.6	85.0	94.1	90.0	88.1	92.2
Average Rank	6.04	7.60	6.68	5.14	4.64	3.94	3.70	4.20	2.56
Number of Top-1	6	0	1	2	4	5	5	3	14
Wins	17	23	23	19	20	15	13	15	-
Draws	4	0	1	2	3	3	4	4	-
Loses	3	2	1	4	2	7	6	3	-

Table 3: Performance comparison with the recent advanced MTSC-dedicated models on 25 UEA datasets. In the table, 'N/A' indicates that the results for the corresponding method could not be obtained due to memory or computational limitations

#### 4.2 Result of UEA Multivariate Datasets

**Setups.** We selected multivariate time series datasets from the UEA Multivariate Time Series Classification Archive. All datasets have been preprocessed and standardized using established preprocessing techniques. To ensure a comprehensive comparison, we incorporated several state-of-the-art baseline methods into our evaluation framework like LSTNet [50], LightTS [51], Rocket [52], LSSL [53], Flowformer [54], MTSMixer [55], TVNet [20], TimeMixer++ [56] on the UEA-10 datasets. Meanwhile, we incorporated WEASEL+MUSE [57], MLSTM-FCN [58], TapNet [59], ShapeNet [60], TodyNet [61], SVPT [62], ShapeFormer [63] and MPTSNet [64] on the UEA-25 datasets, under the same experimental settings.

**Results of UEA-10.** As illustrated in Figure 4, we present the average classification accuracy across ten UEA datasets. It can be observed that SGN surpasses the current best-performing model, TimeMixer++, and consistently outperforms other categories of models. Notably, MLP-based models

exhibit subpar performance on classification tasks, which can be attributed to their lack of explicit modeling of dependencies among variables. In contrast, CNN-based models perform better due to their strong local feature extraction capabilities and ability to capture variable interactions. Complete results are provided in Appendix C.3.

**Results of UEA-25.** Our proposed SGN model consistently demonstrates superior performance across the 25 UEA multivariate time series classification datasets compared with eight state-of-the-art baseline models, as shown in Table 3. It achieves the best average rank of 2.56, the highest number of first-place results (14 datasets), and an overall best win–loss record against all competitors. Notably, SGN outperforms all other models in more than half of the datasets, while maintaining competitive performance in the remaining ones. Furthermore, it exhibits strong generalization ability across diverse domains, including human activity recognition, healthcare, and speech recognition tasks.

#### 4.3 Ablation Studies

**Ablation on Variable Grouping.** To evaluate the effectiveness of our proposed variable grouping strategy, we conduct ablation studies on the main datasets by removing specific components (w/o). The results, as shown in Table 4, demonstrate that performing both intra-group and inter-group interactions outperforms the strategy of directly mixing all variables. This confirms the necessity and effectiveness of our structured variable interaction design. Furthermore, we observe that inter-group interaction yields better performance than intra-group interaction alone, indicating that the model benefits more from capturing diverse dependencies across groups than from modeling redundant information among similar variables.

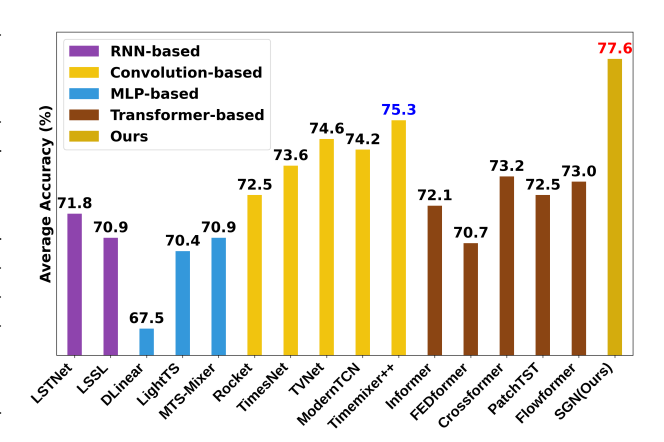


Figure 4: UEA Classification Result of UEA-10 datasets.

Table 4: Ablation Study on Variable Grouping Module across Main Datasets.

Dataset	TDBrain		PTB-XL		FLA	AP	UCI-HAR	
Metric	Accuracy	F1	Accuracy	F1	Accuracy	F1	Accuracy	F1
Variable Group Embedding & Group Interaction	99.90	99.90	73.80	63.43	80.81	80.35	95.62	95.64
w/o Variable Grouping Embedding	92.16	91.64	73.05	62.46	76.85	76.36	93.58	93.58
w/o Group-intra Interaction	99.81	99.81	72.19	61.02	73.82	73.63	91.62	91.69
w/o Group-inter Interaction	99.83	99.83	71.70	60.66	70.60	70.21	88.20	88.15

**Ablation on Periodic Window Shifting and Merging.** This module is designed to validate the effectiveness of extracting features using small periodic windows by leveraging periodic properties. We conduct experiments on the main datasets used in the previous sections, and the detailed results are presented in Table 5. As observed, the impact of periodic fusion is particularly significant, confirming its ability to effectively capture global patterns through multi-period aggregation. Additional ablation studies on hyperparameter sensitivity and efficiency analysis are provided in Appendix D and Appendix E, respectively.

Table 5: Ablation Study on Periodic Window Module across Main Datasets.

Dataset	TDBrain		PTB-	XL	FLA	AΡ	UCI-HAR	
Metric	Accuracy	F1	Accuracy	F1	Accuracy	F1	Accuracy	F1
Periodic Window Shifting & Merging	99.90	99.90	73.80	63.43	80.81	80.35	95.62	95.64
w/o Periodic Window Shifting	99.79	99.79	73.32	62.50	78.05	77.66	87.05	87.22
w/o Periodic Window Merging	99.58	99.58	72.81	62.31	69.68	68.77	77.79	77.83

#### 4.4 Model Analysis.

Analysis of Variable Clustering. As illustrated in Figure 5(a), the initial similarity matrix of variables in the TDBRAIN dataset computed using the BDC distance reveals distinct block structures. These structures indicate inherent similarity among subsets of variables even before model training. Figure 5(b) presents the Pearson correlation matrix computed from the model outputs under the best-performing setting without variable grouping. The results reveal highly diverse and complex relationships among variables, indicating that dependencies exist but are not explicitly structured.

In contrast, Figure 5(c) shows the transformed correlation structure under the variable grouping strategy, where correlations are aggregated at both intra-group and inter-group levels. After training, the intra-group correlations are significantly stronger, suggesting tight dependency within groups, while inter-group correlations are considerably weaker, indicating minimal redundancy across groups. These results demonstrate that variety grouping not only alleviates complex inter-variable dependencies and potential redundancies, but also enhances interpretability and performance in modeling multivariate relationships.

# Analysis of Periodic Shifting and Merging. Figure 6 shows the temporal correlation across SGN layers on the UCI-HAR dataset using learned periodic windows. As observed, in the first layer, the temporal dependencies are primarily concentrated around local neighboring time points.

In contrast, in the last layer, each time point exhibits high correlation with almost all points within the periodic window, demonstrating that SGN effectively integrates hierarchical periodic information. This enables the model to extend the local feature extraction strength of convolutional networks to a global temporal context, enhancing its capacity for comprehensive temporal understanding. Additional visualization results of other main datasets and experimental analyses are provided in Appendix F for further reference.

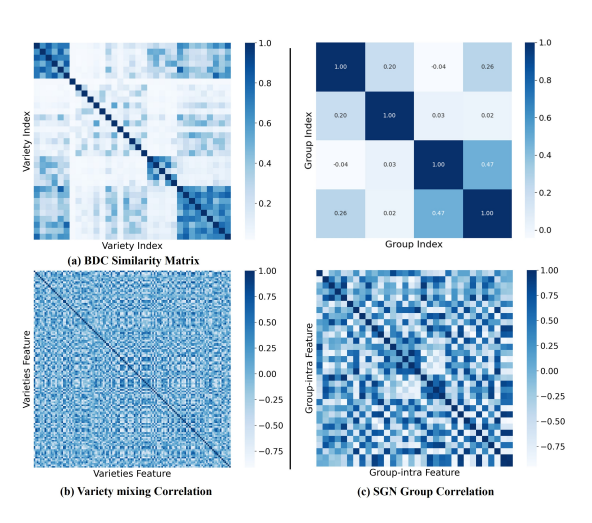


Figure 5: Visualization of TDBRAIN Variety mixing and Variety Grouping matrices.

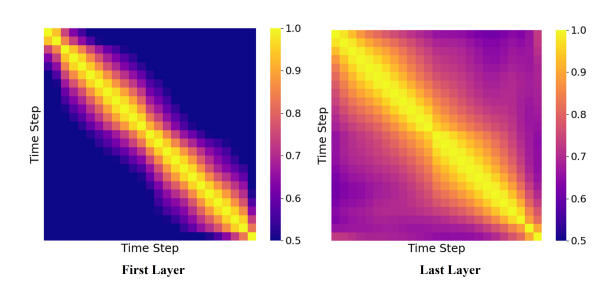


Figure 6: Visualization of time correlation under UCI-HAR dataset.

#### 5 Conclusion

In this paper, we propose SwinGroupNet, a novel and effective framework for multivariate time series (MTS) classification. By leveraging the Variable Group Embedding strategy, we convert variable-level interactions into structured group-based representations. The Multi-Scale Group Window Mixing mechanism further enhances interaction modeling by capturing both intra-group and inter-group dependencies, while simultaneously extracting multi-scale temporal features to enrich temporal representations. Furthermore, the Periodic Window Shifting and Merging approach integrates hierarchical periodic information, enabling the model to better capture dynamic temporal patterns. SGN achieves state-of-the-art performance across diverse datasets spanning multiple domains. Limitations and potential directions for future research are discussed in Appendix G.

# Acknowledgments and Disclosure of Funding

This work was supported in part by the grants from National Natural Science Foundation of China (No.62222213, U22B2059), in part by the Postdoctoral Fellowship Program and China Postdoctoral Science Foundation under Grant Number BX20250387. This work was also supported by USTC-NIO Smart Electric Vehicle Joint Lab.

#### References

- [1] Rafal A. Angryk, Petrus C. Martens, Berkay Aydin, Dustin J. Kempton, Sushant S. Mahajan, Sunitha Basodi, Azim Ahmadzadeh, Xumin Cai, Soukaina Filali Boubrahimi, Shah Muhammad Hamdi, Michael A. Schuh, and Manolis K. Georgoulis. Multivariate time series dataset for space weather data analytics. *Scientific Data*, 2020.
- [2] Markus Reichstein, Gustau Camps-Valls, Bjorn Stevens, Martin Jung, Joachim Denzler, Nuno Carvalhais, and Prabhat. Deep learning and process understanding for data-driven earth system science. *Nat.*, 566(7743):195–204, 2019.
- [3] Yihe Wang, Yu Han, Haishuai Wang, and Xiang Zhang. Contrast everything: A hierarchical contrastive framework for medical time-series. *Advances in Neural Information Processing Systems*, 36, 2024.
- [4] Dominik Klepl, Fei He, Min Wu, Daniel J. Blackburn, and Ptolemaios G. Sarrigiannis. Adaptive gated graph convolutional network for explainable diagnosis of alzheimer's disease using EEG data. *CoRR*, abs/2304.05874, 2023.
- [5] Dani Kiyasseh, Tingting Zhu, and David A. Clifton. CLOCS: contrastive learning of cardiac signals across space, time, and patients. In Marina Meila and Tong Zhang, editors, *Proceedings* of the 38th International Conference on Machine Learning, ICML 2021, 18-24 July 2021, Virtual Event, volume 139 of Proceedings of Machine Learning Research, pages 5606–5615. PMLR, 2021.
- [6] Pavel Filonov, Andrey Lavrentyev, and Artem Vorontsov. Multivariate industrial time series with cyber-attack simulation: Fault detection using an lstm-based predictive data model. *CoRR*, abs/1612.06676, 2016.
- [7] Mohammad Ali Nemer, Joseph Azar, Jacques Demerjian, Abdallah Makhoul, and Julien Bourgeois. A review of research on industrial time series classification for machinery based on deep learning. In 4th IEEE Middle East and North Africa COMMunications Conference, MENACOMM 2022, Amman, Jordan, December 6-8, 2022, pages 89–94. IEEE, 2022.
- [8] Jaeho Kim, Hyewon Kang, Jaewan Yang, Haneul Jung, Seulki Lee, and Junghye Lee. Multi-task deep learning for human activity, speed, and body weight estimation using commercial smart insoles. *IEEE Internet of Things Journal*, 2023.
- [9] Junru Chen, Tianyu Cao, Jing Xu, Jiahe Li, Zhilong Chen, Tao Xiao, and Yang Yang. Con4m: Context-aware consistency learning framework for segmented time series classification. In Amir Globersons, Lester Mackey, Danielle Belgrave, Angela Fan, Ulrich Paquet, Jakub M. Tomczak, and Cheng Zhang, editors, Advances in Neural Information Processing Systems 38: Annual Conference on Neural Information Processing Systems 2024, NeurIPS 2024, Vancouver, BC, Canada, December 10 15, 2024, 2024.
- [10] Zheng Zhao, Weihai Chen, Xingming Wu, Peter CY Chen, and Jingmeng Liu. LSTM network: a deep learning approach for short-term traffic forecast. *IET Intelligent Transport Systems*, 11(2):68–75, 2017.
- [11] Haixu Wu, Jiehui Xu, Jianmin Wang, and Mingsheng Long. Autoformer: Decomposition transformers with auto-correlation for long-term series forecasting. In Marc'Aurelio Ranzato, Alina Beygelzimer, Yann N. Dauphin, Percy Liang, and Jennifer Wortman Vaughan, editors, Advances in Neural Information Processing Systems 34: Annual Conference on Neural Information Processing Systems 2021, NeurIPS 2021, December 6-14, 2021, virtual, pages 22419–22430, 2021.

- [12] Haoyi Zhou, Shanghang Zhang, Jieqi Peng, Shuai Zhang, Jianxin Li, Hui Xiong, and Wancai Zhang. Informer: Beyond efficient transformer for long sequence time-series forecasting. In Thirty-Fifth AAAI Conference on Artificial Intelligence, AAAI 2021, Thirty-Third Conference on Innovative Applications of Artificial Intelligence, IAAI 2021, The Eleventh Symposium on Educational Advances in Artificial Intelligence, EAAI 2021, Virtual Event, February 2-9, 2021, pages 11106–11115. AAAI Press, 2021.
- [13] Yong Liu, Haixu Wu, Jianmin Wang, and Mingsheng Long. Non-stationary transformers: Exploring the stationarity in time series forecasting. In Sanmi Koyejo, S. Mohamed, A. Agarwal, Danielle Belgrave, K. Cho, and A. Oh, editors, *Advances in Neural Information Processing Systems 35: Annual Conference on Neural Information Processing Systems 2022, NeurIPS 2022, New Orleans, LA, USA, November 28 December 9, 2022, 2022.*
- [14] Tian Zhou, Ziqing Ma, Qingsong Wen, Xue Wang, Liang Sun, and Rong Jin. Fedformer: Frequency enhanced decomposed transformer for long-term series forecasting. In Kamalika Chaudhuri, Stefanie Jegelka, Le Song, Csaba Szepesvári, Gang Niu, and Sivan Sabato, editors, International Conference on Machine Learning, ICML 2022, 17-23 July 2022, Baltimore, Maryland, USA, volume 162 of Proceedings of Machine Learning Research, pages 27268– 27286. PMLR, 2022.
- [15] Ailing Zeng, Muxi Chen, Lei Zhang, and Qiang Xu. Are transformers effective for time series forecasting? In Brian Williams, Yiling Chen, and Jennifer Neville, editors, Thirty-Seventh AAAI Conference on Artificial Intelligence, AAAI 2023, Thirty-Fifth Conference on Innovative Applications of Artificial Intelligence, IAAI 2023, Thirteenth Symposium on Educational Advances in Artificial Intelligence, EAAI 2023, Washington, DC, USA, February 7-14, 2023, pages 11121–11128. AAAI Press, 2023.
- [16] Zhe Li, Shiyi Qi, Yiduo Li, and Zenglin Xu. Revisiting long-term time series forecasting: An investigation on linear mapping. *CoRR*, abs/2305.10721, 2023.
- [17] Huiqiang Wang, Jian Peng, Feihu Huang, Jince Wang, Junhui Chen, and Yifei Xiao. MICN: multi-scale local and global context modeling for long-term series forecasting. In *The Eleventh International Conference on Learning Representations, ICLR 2023, Kigali, Rwanda, May 1-5, 2023*. OpenReview.net, 2023.
- [18] Haixu Wu, Tengge Hu, Yong Liu, Hang Zhou, Jianmin Wang, and Mingsheng Long. Timesnet: Temporal 2d-variation modeling for general time series analysis. In *The Eleventh International Conference on Learning Representations, ICLR 2023, Kigali, Rwanda, May 1-5, 2023*. OpenReview.net, 2023.
- [19] Donghao Luo and Xue Wang. Moderntcn: A modern pure convolution structure for general time series analysis. In *The Twelfth International Conference on Learning Representations, ICLR 2024, Vienna, Austria, May 7-11, 2024*. OpenReview.net, 2024.
- [20] Chenghan Li, Mingchen Li, and Ruisheng Diao. TVNet: A novel time series analysis method based on dynamic convolution and 3d-variation. In *The Thirteenth International Conference on Learning Representations*, 2025.
- [21] Ao Wang, Hui Chen, Zijia Lin, Hengjun Pu, and Guiguang Ding. Repvit: Revisiting mobile CNN from vit perspective. *CoRR*, abs/2307.09283, 2023.
- [22] Yuqi Nie, Nam H. Nguyen, Phanwadee Sinthong, and Jayant Kalagnanam. A time series is worth 64 words: Long-term forecasting with transformers. In *The Eleventh International Conference on Learning Representations, ICLR 2023, Kigali, Rwanda, May 1-5, 2023*. OpenReview.net, 2023.
- [23] Jaeho Kim, Seok-Ju Hahn, Yoontae Hwang, Junghye Lee, and Seulki Lee. CAFO: feature-centric explanation on time series classification. In Ricardo Baeza-Yates and Francesco Bonchi, editors, *Proceedings of the 30th ACM SIGKDD Conference on Knowledge Discovery and Data Mining, KDD 2024, Barcelona, Spain, August 25-29, 2024*, pages 1372–1382. ACM, 2024.

- [24] Yong Liu, Tengge Hu, Haoran Zhang, Haixu Wu, Shiyu Wang, Lintao Ma, and Mingsheng Long. itransformer: Inverted transformers are effective for time series forecasting. In *The Twelfth International Conference on Learning Representations, ICLR 2024, Vienna, Austria, May 7-11, 2024*. OpenReview.net, 2024.
- [25] Yunhao Zhang and Junchi Yan. Crossformer: Transformer utilizing cross-dimension dependency for multivariate time series forecasting. In *The Eleventh International Conference on Learning Representations, ICLR 2023, Kigali, Rwanda, May 1-5, 2023.* OpenReview.net, 2023.
- [26] Shoaib Ahmed Siddiqui, Dominique Mercier, Mohsin Munir, Andreas Dengel, and Sheraz Ahmed. Tsviz: Demystification of deep learning models for time-series analysis. *IEEE Access*, 7:67027–67040, 2019.
- [27] Jialin Chen, Jan Eric Lenssen, Aosong Feng, Weihua Hu, Matthias Fey, Leandros Tassiulas, Jure Leskovec, and Rex Ying. From similarity to superiority: Channel clustering for time series forecasting. In Amir Globersons, Lester Mackey, Danielle Belgrave, Angela Fan, Ulrich Paquet, Jakub M. Tomczak, and Cheng Zhang, editors, Advances in Neural Information Processing Systems 38: Annual Conference on Neural Information Processing Systems 2024, NeurIPS 2024, Vancouver, BC, Canada, December 10 15, 2024, 2024.
- [28] Shaojie Bai, J. Zico Kolter, and Vladlen Koltun. An empirical evaluation of generic convolutional and recurrent networks for sequence modeling. *CoRR*, abs/1803.01271, 2018.
- [29] Rajat Sen, Hsiang-Fu Yu, and Inderjit S. Dhillon. Think globally, act locally: A deep neural network approach to high-dimensional time series forecasting. In Hanna M. Wallach, Hugo Larochelle, Alina Beygelzimer, Florence d'Alché-Buc, Emily B. Fox, and Roman Garnett, editors, Advances in Neural Information Processing Systems 32: Annual Conference on Neural Information Processing Systems 2019, NeurIPS 2019, December 8-14, 2019, Vancouver, BC, Canada, pages 4838–4847, 2019.
- [30] Qihe Huang, Lei Shen, Ruixin Zhang, Shouhong Ding, Binwu Wang, Zhengyang Zhou, and Yang Wang. Crossgnn: Confronting noisy multivariate time series via cross interaction refinement. In Alice Oh, Tristan Naumann, Amir Globerson, Kate Saenko, Moritz Hardt, and Sergey Levine, editors, Advances in Neural Information Processing Systems 36: Annual Conference on Neural Information Processing Systems 2023, NeurIPS 2023, New Orleans, LA, USA, December 10 - 16, 2023, 2023.
- [31] Peiwen Yuan and Changsheng Zhu. Is channel independent strategy optimal for time series forecasting? *CoRR*, abs/2310.17658, 2023.
- [32] Lu Han, Han-Jia Ye, and De-Chuan Zhan. The capacity and robustness trade-off: Revisiting the channel independent strategy for multivariate time series forecasting. *IEEE Trans. Knowl. Data Eng.*, 36(11):7129–7142, 2024.
- [33] Pablo Montero-Manso and Rob J. Hyndman. Principles and algorithms for forecasting groups of time series: Locality and globality. *CoRR*, abs/2008.00444, 2020.
- [34] Xue Wang, Tian Zhou, Qingsong Wen, Jinyang Gao, Bolin Ding, and Rong Jin. CARD: channel aligned robust blend transformer for time series forecasting. In *The Twelfth International Conference on Learning Representations, ICLR 2024, Vienna, Austria, May 7-11, 2024*. OpenReview.net, 2024.
- [35] Jung-Yi Jiang, Ren-Jia Liou, and Shie-Jue Lee. A fuzzy self-constructing feature clustering algorithm for text classification. *IEEE Trans. Knowl. Data Eng.*, 23(3):335–349, 2011.
- [36] Dmitrii Marin, Jen-Hao Rick Chang, Anurag Ranjan, Anish Prabhu, Mohammad Rastegari, and Oncel Tuzel. Token pooling in vision transformers for image classification. In *IEEE/CVF Winter Conference on Applications of Computer Vision, WACV 2023, Waikoloa, HI, USA, January 2-7, 2023*, pages 12–21. IEEE, 2023.
- [37] Hao Li, Alin Achim, and David R. Bull. Unsupervised video anomaly detection using feature clustering. *IET Signal Process.*, 6(5):521–533, 2012.

- [38] Lijimol George and P Sumathy. An integrated clustering and bert framework for improved topic modeling. *International Journal of Information Technology*, pages 1–9, 2023.
- [39] Eric Jang, Shixiang Gu, and Ben Poole. Categorical reparameterization with gumbel-softmax. In 5th International Conference on Learning Representations, ICLR 2017, Toulon, France, April 24-26, 2017, Conference Track Proceedings. OpenReview.net, 2017.
- [40] Chris J. Maddison, Andriy Mnih, and Yee Whye Teh. The concrete distribution: A continuous relaxation of discrete random variables. In 5th International Conference on Learning Representations, ICLR 2017, Toulon, France, April 24-26, 2017, Conference Track Proceedings. OpenReview.net, 2017.
- [41] Gábor J Székely, Maria L Rizzo, and Nail K Bakirov. Measuring and testing dependence by correlation of distances. *The Annals of Statistics*, 35(6):2769–2794, 2007.
- [42] Zhuang Liu, Hanzi Mao, Chao-Yuan Wu, Christoph Feichtenhofer, Trevor Darrell, and Saining Xie. A convnet for the 2020s. In *Proceedings of the IEEE/CVF Conference on Computer Vision and Pattern Recognition (CVPR)*, pages 11976–11986, 2022.
- [43] Yazan Abu Farha and Jürgen Gall. MS-TCN: multi-stage temporal convolutional network for action segmentation. In *IEEE Conference on Computer Vision and Pattern Recognition, CVPR 2019, Long Beach, CA, USA, June 16-20, 2019*, pages 3575–3584. Computer Vision Foundation / IEEE, 2019.
- [44] Liu Che, Tong Xu, Qi Liu, Zhi Zheng, Jingyu Peng, and Enhong Chen. MERGE: multi-view relationship graph network for event-driven stock movement prediction. In Wenjie Zhang, Anthony K. H. Tung, Zhonglong Zheng, Zhengyi Yang, Xiaoyang Wang, and Hongjie Guo, editors, Web and Big Data 8th International Joint Conference, APWeb-WAIM 2024, Jinhua, China, August 30 September 1, 2024, Proceedings, Part III, volume 14963 of Lecture Notes in Computer Science, pages 224–239. Springer, 2024.
- [45] Qi Liu, Jingqing Ruan, Hao Li, Haodong Zhao, Desheng Wang, Jiansong Chen, Wan Guanglu, Xunliang Cai, Zhi Zheng, and Tong Xu. AMoPO: Adaptive multi-objective preference optimization without reward models and reference models. In Wanxiang Che, Joyce Nabende, Ekaterina Shutova, and Mohammad Taher Pilehvar, editors, *Findings of the Association for Computational Linguistics: ACL 2025*, pages 8832–8866, Vienna, Austria, July 2025. Association for Computational Linguistics.
- [46] Ze Liu, Yutong Lin, Yue Cao, Han Hu, Yixuan Wei, Zheng Zhang, Stephen Lin, and Baining Guo. Swin transformer: Hierarchical vision transformer using shifted windows. In 2021 IEEE/CVF International Conference on Computer Vision, ICCV 2021, Montreal, QC, Canada, October 10-17, 2021, pages 9992–10002. IEEE, 2021.
- [47] Anthony J. Bagnall, Hoang Anh Dau, Jason Lines, Michael Flynn, James Large, Aaron Bostrom, Paul Southam, and Eamonn J. Keogh. The UEA multivariate time series classification archive, 2018. CoRR, abs/1811.00075, 2018.
- [48] Nikita Kitaev, Lukasz Kaiser, and Anselm Levskaya. Reformer: The efficient transformer. In 8th International Conference on Learning Representations, ICLR 2020, Addis Ababa, Ethiopia, April 26-30, 2020. OpenReview.net, 2020.
- [49] Yihe Wang, Nan Huang, Taida Li, Yujun Yan, and Xiang Zhang. Medformer: A multi-granularity patching transformer for medical time-series classification. In Amir Globersons, Lester Mackey, Danielle Belgrave, Angela Fan, Ulrich Paquet, Jakub M. Tomczak, and Cheng Zhang, editors, Advances in Neural Information Processing Systems 38: Annual Conference on Neural Information Processing Systems 2024, NeurIPS 2024, Vancouver, BC, Canada, December 10 15, 2024, 2024.
- [50] Guokun Lai, Wei-Cheng Chang, Yiming Yang, and Hanxiao Liu. Modeling long- and short-term temporal patterns with deep neural networks. In Kevyn Collins-Thompson, Qiaozhu Mei, Brian D. Davison, Yiqun Liu, and Emine Yilmaz, editors, *The 41st International ACM SIGIR Conference on Research & Development in Information Retrieval, SIGIR 2018, Ann Arbor, MI, USA, July 08-12, 2018*, pages 95–104. ACM, 2018.

- [51] Tianping Zhang, Yizhuo Zhang, Wei Cao, Jiang Bian, Xiaohan Yi, Shun Zheng, and Jian Li. Less is more: Fast multivariate time series forecasting with light sampling-oriented MLP structures. CoRR, abs/2207.01186, 2022.
- [52] Angus Dempster, François Petitjean, and Geoffrey I. Webb. ROCKET: exceptionally fast and accurate time series classification using random convolutional kernels. *Data Min. Knowl. Discov.*, 34(5):1454–1495, 2020.
- [53] Albert Gu, Karan Goel, and Christopher Ré. Efficiently modeling long sequences with structured state spaces. In *The Tenth International Conference on Learning Representations, ICLR* 2022, *Virtual Event, April* 25-29, 2022. OpenReview.net, 2022.
- [54] Haixu Wu, Jialong Wu, Jiehui Xu, Jianmin Wang, and Mingsheng Long. Flowformer: Linearizing transformers with conservation flows. In Kamalika Chaudhuri, Stefanie Jegelka, Le Song, Csaba Szepesvári, Gang Niu, and Sivan Sabato, editors, *International Conference on Machine Learning, ICML* 2022, 17-23 July 2022, Baltimore, Maryland, USA, volume 162 of Proceedings of Machine Learning Research, pages 24226–24242. PMLR, 2022.
- [55] Zhe Li, Zhongwen Rao, Lujia Pan, and Zenglin Xu. Mts-mixers: Multivariate time series forecasting via factorized temporal and channel mixing. *CoRR*, abs/2302.04501, 2023.
- [56] Shiyu Wang, Jiawei LI, Xiaoming Shi, Zhou Ye, Baichuan Mo, Wenze Lin, Ju Shengtong, Zhixuan Chu, and Ming Jin. Timemixer++: A general time series pattern machine for universal predictive analysis. In *The Thirteenth International Conference on Learning Representations*, 2025.
- [57] Patrick Schäfer and Ulf Leser. Multivariate time series classification with WEASEL+MUSE. *CoRR*, abs/1711.11343, 2017.
- [58] Fazle Karim, Somshubra Majumdar, Houshang Darabi, and Samuel Harford. Multivariate lstm-fcns for time series classification. *Neural Networks*, 116:237–245, 2019.
- [59] Xuchao Zhang, Yifeng Gao, Jessica Lin, and Chang-Tien Lu. Tapnet: Multivariate time series classification with attentional prototypical network. In The Thirty-Fourth AAAI Conference on Artificial Intelligence, AAAI 2020, The Thirty-Second Innovative Applications of Artificial Intelligence Conference, IAAI 2020, The Tenth AAAI Symposium on Educational Advances in Artificial Intelligence, EAAI 2020, New York, NY, USA, February 7-12, 2020, pages 6845–6852. AAAI Press, 2020.
- [60] Guozhong Li, Byron Choi, Jianliang Xu, Sourav S. Bhowmick, Kwok-Pan Chun, and Grace Lai-Hung Wong. Shapenet: A shapelet-neural network approach for multivariate time series classification. In Thirty-Fifth AAAI Conference on Artificial Intelligence, AAAI 2021, Thirty-Third Conference on Innovative Applications of Artificial Intelligence, IAAI 2021, The Eleventh Symposium on Educational Advances in Artificial Intelligence, EAAI 2021, Virtual Event, February 2-9, 2021, pages 8375–8383. AAAI Press, 2021.
- [61] Huaiyuan Liu, Donghua Yang, Xianzhang Liu, Xinglei Chen, Zhiyu Liang, Hongzhi Wang, Yong Cui, and Jun Gu. Todynet: Temporal dynamic graph neural network for multivariate time series classification. *Inf. Sci.*, 677:120914, 2024.
- [62] Rundong Zuo, Guozhong Li, Byron Choi, Sourav S. Bhowmick, Daphne Ngar-yin Mah, and Grace Lai-Hung Wong. SVP-T: A shape-level variable-position transformer for multivariate time series classification. In Brian Williams, Yiling Chen, and Jennifer Neville, editors, Thirty-Seventh AAAI Conference on Artificial Intelligence, AAAI 2023, Thirty-Fifth Conference on Innovative Applications of Artificial Intelligence, IAAI 2023, Thirteenth Symposium on Educational Advances in Artificial Intelligence, EAAI 2023, Washington, DC, USA, February 7-14, 2023, pages 11497–11505. AAAI Press, 2023.
- [63] Xuan-May Le, Ling Luo, Uwe Aickelin, and Minh-Tuan Tran. Shapeformer: Shapelet transformer for multivariate time series classification. In Ricardo Baeza-Yates and Francesco Bonchi, editors, Proceedings of the 30th ACM SIGKDD Conference on Knowledge Discovery and Data Mining, KDD 2024, Barcelona, Spain, August 25-29, 2024, pages 1484–1494. ACM, 2024.

- [64] Yang Mu, Muhammad Shahzad, and Xiao Xiang Zhu. Mptsnet: Integrating multiscale periodic local patterns and global dependencies for multivariate time series classification. In Toby Walsh, Julie Shah, and Zico Kolter, editors, AAAI-25, Sponsored by the Association for the Advancement of Artificial Intelligence, February 25 March 4, 2025, Philadelphia, PA, USA, pages 19572–19580. AAAI Press, 2025.
- [65] Stuart P. Lloyd. Least squares quantization in PCM. IEEE Trans. Inf. Theory, 28(2):129–136, 1982.
- [66] Hanneke van Dijk, Guido van Wingen, Damiaan Denys, Sebastian Olbrich, Rosalinde van Ruth, and Martijn Arns. The two decades brainclinics research archive for insights in neurophysiology (tdbrain) database. *Scientific Data*, 9(1):333, 2022.
- [67] Patrick Wagner, Nils Strodthoff, Ralf-Dieter Bousseljot, Dieter Kreiseler, Fatima I Lunze, Wojciech Samek, and Tobias Schaeffter. Ptb-xl: A large publicly available electrocardiography dataset. *Scientific Data*, 7(1):1–15, 2020.
- [68] Prabhat Kumar and S Suresh. Flaap: An open human activity recognition (har) dataset for learning and finding the associated activity patterns. *Procedia Computer Science*, 212:64–73, 2022.
- [69] Davide Anguita, Alessandro Ghio, Luca Oneto, Xavier Parra, Jorge Luis Reyes-Ortiz, et al. A public domain dataset for human activity recognition using smartphones. In *European Symposium on Artificial Neural Networks (ESANN)*, volume 3, page 3, 2013.
- [70] Diederik P. Kingma and Jimmy Ba. Adam: A method for stochastic optimization. In Yoshua Bengio and Yann LeCun, editors, 3rd International Conference on Learning Representations, ICLR 2015, San Diego, CA, USA, May 7-9, 2015, Conference Track Proceedings, 2015.
- [71] Adam Paszke, Sam Gross, Francisco Massa, Adam Lerer, James Bradbury, Gregory Chanan, Trevor Killeen, Zeming Lin, Natalia Gimelshein, Luca Antiga, Alban Desmaison, Andreas Köpf, Edward Z. Yang, Zachary DeVito, Martin Raison, Alykhan Tejani, Sasank Chilamkurthy, Benoit Steiner, Lu Fang, Junjie Bai, and Soumith Chintala. Pytorch: An imperative style, high-performance deep learning library. In Hanna M. Wallach, Hugo Larochelle, Alina Beygelzimer, Florence d'Alché-Buc, Emily B. Fox, and Roman Garnett, editors, Advances in Neural Information Processing Systems 32: Annual Conference on Neural Information Processing Systems 2019, NeurIPS 2019, December 8-14, 2019, Vancouver, BC, Canada, pages 8024–8035, 2019.

# **NeurIPS Paper Checklist**

The checklist is designed to encourage best practices for responsible machine learning research, addressing issues of reproducibility, transparency, research ethics, and societal impact. Do not remove the checklist: **The papers not including the checklist will be desk rejected.** The checklist should follow the references and follow the (optional) supplemental material. The checklist does NOT count towards the page limit.

Please read the checklist guidelines carefully for information on how to answer these questions. For each question in the checklist:

- You should answer [Yes], [No], or [NA].
- [NA] means either that the question is Not Applicable for that particular paper or the relevant information is Not Available.
- Please provide a short (1–2 sentence) justification right after your answer (even for NA).

The checklist answers are an integral part of your paper submission. They are visible to the reviewers, area chairs, senior area chairs, and ethics reviewers. You will be asked to also include it (after eventual revisions) with the final version of your paper, and its final version will be published with the paper.

The reviewers of your paper will be asked to use the checklist as one of the factors in their evaluation. While "[Yes]" is generally preferable to "[No]", it is perfectly acceptable to answer "[No]" provided a proper justification is given (e.g., "error bars are not reported because it would be too computationally expensive" or "we were unable to find the license for the dataset we used"). In general, answering "[No]" or "[NA]" is not grounds for rejection. While the questions are phrased in a binary way, we acknowledge that the true answer is often more nuanced, so please just use your best judgment and write a justification to elaborate. All supporting evidence can appear either in the main paper or the supplemental material, provided in appendix. If you answer [Yes] to a question, in the justification please point to the section(s) where related material for the question can be found.

# IMPORTANT, please:

- Delete this instruction block, but keep the section heading "NeurIPS Paper Checklist",
- Keep the checklist subsection headings, questions/answers and guidelines below.
- Do not modify the questions and only use the provided macros for your answers.

# 1. Claims

Question: Do the main claims made in the abstract and introduction accurately reflect the paper's contributions and scope?

Answer: [Yes]

Justification: Clearly state the contribution in the introduction.

#### Guidelines:

- The answer NA means that the abstract and introduction do not include the claims made in the paper.
- The abstract and/or introduction should clearly state the claims made, including the contributions made in the paper and important assumptions and limitations. A No or NA answer to this question will not be perceived well by the reviewers.
- The claims made should match theoretical and experimental results, and reflect how much the results can be expected to generalize to other settings.
- It is fine to include aspirational goals as motivation as long as it is clear that these goals are not attained by the paper.

#### 2. Limitations

Question: Does the paper discuss the limitations of the work performed by the authors?

Answer: [Yes]

Justification: See Appendix G.

#### Guidelines:

- The answer NA means that the paper has no limitation while the answer No means that the paper has limitations, but those are not discussed in the paper.
- The authors are encouraged to create a separate "Limitations" section in their paper.
- The paper should point out any strong assumptions and how robust the results are to violations of these assumptions (e.g., independence assumptions, noiseless settings, model well-specification, asymptotic approximations only holding locally). The authors should reflect on how these assumptions might be violated in practice and what the implications would be.
- The authors should reflect on the scope of the claims made, e.g., if the approach was only tested on a few datasets or with a few runs. In general, empirical results often depend on implicit assumptions, which should be articulated.
- The authors should reflect on the factors that influence the performance of the approach. For example, a facial recognition algorithm may perform poorly when image resolution is low or images are taken in low lighting. Or a speech-to-text system might not be used reliably to provide closed captions for online lectures because it fails to handle technical jargon.
- The authors should discuss the computational efficiency of the proposed algorithms and how they scale with dataset size.
- If applicable, the authors should discuss possible limitations of their approach to address problems of privacy and fairness.
- While the authors might fear that complete honesty about limitations might be used by reviewers as grounds for rejection, a worse outcome might be that reviewers discover limitations that aren't acknowledged in the paper. The authors should use their best judgment and recognize that individual actions in favor of transparency play an important role in developing norms that preserve the integrity of the community. Reviewers will be specifically instructed to not penalize honesty concerning limitations.

#### 3. Theory assumptions and proofs

Question: For each theoretical result, does the paper provide the full set of assumptions and a complete (and correct) proof?

Answer: [NA]

Justification: This paper does not include theoretical results.

#### Guidelines:

- The answer NA means that the paper does not include theoretical results.
- All the theorems, formulas, and proofs in the paper should be numbered and crossreferenced.
- All assumptions should be clearly stated or referenced in the statement of any theorems.
- The proofs can either appear in the main paper or the supplemental material, but if they appear in the supplemental material, the authors are encouraged to provide a short proof sketch to provide intuition.
- Inversely, any informal proof provided in the core of the paper should be complemented by formal proofs provided in appendix or supplemental material.
- Theorems and Lemmas that the proof relies upon should be properly referenced.

#### 4. Experimental result reproducibility

Question: Does the paper fully disclose all the information needed to reproduce the main experimental results of the paper to the extent that it affects the main claims and/or conclusions of the paper (regardless of whether the code and data are provided or not)?

Answer: [Yes]

Justification: See Section 4 and Appendix C.

#### Guidelines:

• The answer NA means that the paper does not include experiments.

- If the paper includes experiments, a No answer to this question will not be perceived well by the reviewers: Making the paper reproducible is important, regardless of whether the code and data are provided or not.
- If the contribution is a dataset and/or model, the authors should describe the steps taken to make their results reproducible or verifiable.
- Depending on the contribution, reproducibility can be accomplished in various ways. For example, if the contribution is a novel architecture, describing the architecture fully might suffice, or if the contribution is a specific model and empirical evaluation, it may be necessary to either make it possible for others to replicate the model with the same dataset, or provide access to the model. In general, releasing code and data is often one good way to accomplish this, but reproducibility can also be provided via detailed instructions for how to replicate the results, access to a hosted model (e.g., in the case of a large language model), releasing of a model checkpoint, or other means that are appropriate to the research performed.
- While NeurIPS does not require releasing code, the conference does require all submissions to provide some reasonable avenue for reproducibility, which may depend on the nature of the contribution. For example
  - (a) If the contribution is primarily a new algorithm, the paper should make it clear how to reproduce that algorithm.
- (b) If the contribution is primarily a new model architecture, the paper should describe the architecture clearly and fully.
- (c) If the contribution is a new model (e.g., a large language model), then there should either be a way to access this model for reproducing the results or a way to reproduce the model (e.g., with an open-source dataset or instructions for how to construct the dataset).
- (d) We recognize that reproducibility may be tricky in some cases, in which case authors are welcome to describe the particular way they provide for reproducibility. In the case of closed-source models, it may be that access to the model is limited in some way (e.g., to registered users), but it should be possible for other researchers to have some path to reproducing or verifying the results.

# 5. Open access to data and code

Question: Does the paper provide open access to the data and code, with sufficient instructions to faithfully reproduce the main experimental results, as described in supplemental material?

Answer: [Yes]

Justification: We include a github link in the Abstract providing source codes with full implementation details for our methods. All datasets used for evaluation are publicly available.

- The answer NA means that paper does not include experiments requiring code.
- Please see the NeurIPS code and data submission guidelines (https://nips.cc/public/guides/CodeSubmissionPolicy) for more details.
- While we encourage the release of code and data, we understand that this might not be possible, so "No" is an acceptable answer. Papers cannot be rejected simply for not including code, unless this is central to the contribution (e.g., for a new open-source benchmark).
- The instructions should contain the exact command and environment needed to run to reproduce the results. See the NeurIPS code and data submission guidelines (https://nips.cc/public/guides/CodeSubmissionPolicy) for more details.
- The authors should provide instructions on data access and preparation, including how to access the raw data, preprocessed data, intermediate data, and generated data, etc.
- The authors should provide scripts to reproduce all experimental results for the new proposed method and baselines. If only a subset of experiments are reproducible, they should state which ones are omitted from the script and why.
- At submission time, to preserve anonymity, the authors should release anonymized versions (if applicable).

• Providing as much information as possible in supplemental material (appended to the paper) is recommended, but including URLs to data and code is permitted.

#### 6. Experimental setting/details

Question: Does the paper specify all the training and test details (e.g., data splits, hyperparameters, how they were chosen, type of optimizer, etc.) necessary to understand the results?

Answer: [Yes]

Justification: See Appendix C

#### Guidelines:

- The answer NA means that the paper does not include experiments.
- The experimental setting should be presented in the core of the paper to a level of detail that is necessary to appreciate the results and make sense of them.
- The full details can be provided either with the code, in appendix, or as supplemental
  material.

#### 7. Experiment statistical significance

Question: Does the paper report error bars suitably and correctly defined or other appropriate information about the statistical significance of the experiments?

Answer: [Yes]

Justification: We run experiments over five random seeds and report the average value with the standard deviation. See Table 2

#### Guidelines:

- The answer NA means that the paper does not include experiments.
- The authors should answer "Yes" if the results are accompanied by error bars, confidence intervals, or statistical significance tests, at least for the experiments that support the main claims of the paper.
- The factors of variability that the error bars are capturing should be clearly stated (for example, train/test split, initialization, random drawing of some parameter, or overall run with given experimental conditions).
- The method for calculating the error bars should be explained (closed form formula, call to a library function, bootstrap, etc.)
- The assumptions made should be given (e.g., Normally distributed errors).
- It should be clear whether the error bar is the standard deviation or the standard error
  of the mean.
- It is OK to report 1-sigma error bars, but one should state it. The authors should preferably report a 2-sigma error bar than state that they have a 96% CI, if the hypothesis of Normality of errors is not verified.
- For asymmetric distributions, the authors should be careful not to show in tables or figures symmetric error bars that would yield results that are out of range (e.g. negative error rates).
- If error bars are reported in tables or plots, The authors should explain in the text how they were calculated and reference the corresponding figures or tables in the text.

#### 8. Experiments compute resources

Question: For each experiment, does the paper provide sufficient information on the computer resources (type of compute workers, memory, time of execution) needed to reproduce the experiments?

Answer: [Yes]

Justification: See Appendix C.1

- The answer NA means that the paper does not include experiments.
- The paper should indicate the type of compute workers CPU or GPU, internal cluster, or cloud provider, including relevant memory and storage.

- The paper should provide the amount of compute required for each of the individual experimental runs as well as estimate the total compute.
- The paper should disclose whether the full research project required more compute than the experiments reported in the paper (e.g., preliminary or failed experiments that didn't make it into the paper).

#### 9. Code of ethics

Question: Does the research conducted in the paper conform, in every respect, with the NeurIPS Code of Ethics https://neurips.cc/public/EthicsGuidelines?

Answer: [Yes]

Justification: The authors follow the NeurIPS Code of Ethics during the conduct of this research.

#### Guidelines:

- The answer NA means that the authors have not reviewed the NeurIPS Code of Ethics.
- If the authors answer No, they should explain the special circumstances that require a
  deviation from the Code of Ethics.
- The authors should make sure to preserve anonymity (e.g., if there is a special consideration due to laws or regulations in their jurisdiction).

#### 10. Broader impacts

Question: Does the paper discuss both potential positive societal impacts and negative societal impacts of the work performed?

Answer: [Yes]

Justification: See Appendix G

#### Guidelines:

- The answer NA means that there is no societal impact of the work performed.
- If the authors answer NA or No, they should explain why their work has no societal impact or why the paper does not address societal impact.
- Examples of negative societal impacts include potential malicious or unintended uses (e.g., disinformation, generating fake profiles, surveillance), fairness considerations (e.g., deployment of technologies that could make decisions that unfairly impact specific groups), privacy considerations, and security considerations.
- The conference expects that many papers will be foundational research and not tied to particular applications, let alone deployments. However, if there is a direct path to any negative applications, the authors should point it out. For example, it is legitimate to point out that an improvement in the quality of generative models could be used to generate deepfakes for disinformation. On the other hand, it is not needed to point out that a generic algorithm for optimizing neural networks could enable people to train models that generate Deepfakes faster.
- The authors should consider possible harms that could arise when the technology is being used as intended and functioning correctly, harms that could arise when the technology is being used as intended but gives incorrect results, and harms following from (intentional or unintentional) misuse of the technology.
- If there are negative societal impacts, the authors could also discuss possible mitigation strategies (e.g., gated release of models, providing defenses in addition to attacks, mechanisms for monitoring misuse, mechanisms to monitor how a system learns from feedback over time, improving the efficiency and accessibility of ML).

# 11. Safeguards

Question: Does the paper describe safeguards that have been put in place for responsible release of data or models that have a high risk for misuse (e.g., pretrained language models, image generators, or scraped datasets)?

Answer: [NA]

Justification: this paper poses no such risks.

- The answer NA means that the paper poses no such risks.
- Released models that have a high risk for misuse or dual-use should be released with necessary safeguards to allow for controlled use of the model, for example by requiring that users adhere to usage guidelines or restrictions to access the model or implementing safety filters.
- Datasets that have been scraped from the Internet could pose safety risks. The authors should describe how they avoided releasing unsafe images.
- We recognize that providing effective safeguards is challenging, and many papers do
  not require this, but we encourage authors to take this into account and make a best
  faith effort.

#### 12. Licenses for existing assets

Question: Are the creators or original owners of assets (e.g., code, data, models), used in the paper, properly credited and are the license and terms of use explicitly mentioned and properly respected?

Answer: [Yes]

Justification: Cited the original paper that produced the dataset used in this work.

#### Guidelines:

- The answer NA means that the paper does not use existing assets.
- The authors should cite the original paper that produced the code package or dataset.
- The authors should state which version of the asset is used and, if possible, include a URL.
- The name of the license (e.g., CC-BY 4.0) should be included for each asset.
- For scraped data from a particular source (e.g., website), the copyright and terms of service of that source should be provided.
- If assets are released, the license, copyright information, and terms of use in the package should be provided. For popular datasets, paperswithcode.com/datasets has curated licenses for some datasets. Their licensing guide can help determine the license of a dataset.
- For existing datasets that are re-packaged, both the original license and the license of the derived asset (if it has changed) should be provided.
- If this information is not available online, the authors are encouraged to reach out to the asset's creators.

#### 13. New assets

Question: Are new assets introduced in the paper well documented and is the documentation provided alongside the assets?

Answer: [NA]

Justification: This paper does not publish new assets.

#### Guidelines:

- The answer NA means that the paper does not release new assets.
- Researchers should communicate the details of the dataset/code/model as part of their submissions via structured templates. This includes details about training, license, limitations, etc.
- The paper should discuss whether and how consent was obtained from people whose asset is used.
- At submission time, remember to anonymize your assets (if applicable). You can either create an anonymized URL or include an anonymized zip file.

# 14. Crowdsourcing and research with human subjects

Question: For crowdsourcing experiments and research with human subjects, does the paper include the full text of instructions given to participants and screenshots, if applicable, as well as details about compensation (if any)?

Answer: [NA]

Justification: This paper does not involve crowdsourcing nor research with human subjects. Guidelines:

- The answer NA means that the paper does not involve crowdsourcing nor research with human subjects.
- Including this information in the supplemental material is fine, but if the main contribution of the paper involves human subjects, then as much detail as possible should be included in the main paper.
- According to the NeurIPS Code of Ethics, workers involved in data collection, curation, or other labor should be paid at least the minimum wage in the country of the data collector

# 15. Institutional review board (IRB) approvals or equivalent for research with human subjects

Question: Does the paper describe potential risks incurred by study participants, whether such risks were disclosed to the subjects, and whether Institutional Review Board (IRB) approvals (or an equivalent approval/review based on the requirements of your country or institution) were obtained?

Answer: [NA]

Justification: This paper does not involve crowdsourcing nor research with human subjects. Guidelines:

- The answer NA means that the paper does not involve crowdsourcing nor research with human subjects.
- Depending on the country in which research is conducted, IRB approval (or equivalent) may be required for any human subjects research. If you obtained IRB approval, you should clearly state this in the paper.
- We recognize that the procedures for this may vary significantly between institutions and locations, and we expect authors to adhere to the NeurIPS Code of Ethics and the guidelines for their institution.
- For initial submissions, do not include any information that would break anonymity (if applicable), such as the institution conducting the review.

#### 16. Declaration of LLM usage

Question: Does the paper describe the usage of LLMs if it is an important, original, or non-standard component of the core methods in this research? Note that if the LLM is used only for writing, editing, or formatting purposes and does not impact the core methodology, scientific rigorousness, or originality of the research, declaration is not required.

Answer: [NA]

Justification: This paper does not use LLMs in the core method development.

- The answer NA means that the core method development in this research does not involve LLMs as any important, original, or non-standard components.
- Please refer to our LLM policy (https://neurips.cc/Conferences/2025/LLM) for what should or should not be described.

# A Variety Assign Logits

Previous studies commonly adopt the *Pearson correlation coefficient* to measure dependencies between variables, which is effective for capturing linear relationships. The Pearson correlation between two variables  $\mathbf{x}, \mathbf{y} \in \mathbb{R}^n$  is defined as:

$$\rho(\mathbf{x}, \mathbf{y}) = \frac{\sum_{i=1}^{n} (x_i - \bar{x})(y_i - \bar{y})}{\sqrt{\sum_{i=1}^{n} (x_i - \bar{x})^2} \cdot \sqrt{\sum_{i=1}^{n} (y_i - \bar{y})^2}},$$
(8)

where  $\bar{x}$  and  $\bar{y}$  denote the sample means of x and y, respectively. While this approach performs well under linear assumptions, it fails to capture complex nonlinear dependencies—an issue particularly prominent in multivariate time series, where variable interactions can be intricate and highly nonlinear.

To address this limitation, we adopt the *Brownian Distance Covariance (BDC)* as an alternative. Unlike Pearson correlation, BDC is a nonparametric statistical measure that can detect both linear and nonlinear dependencies without assuming any specific distribution. It provides a more general and powerful tool for modeling complex interactions in multivariate time series. The empirical BDC between x and y is defined as:

$$\mathcal{R}_n(\mathbf{x}, \mathbf{y}) = \frac{\mathcal{V}_n(\mathbf{x}, \mathbf{y})}{\sqrt{\mathcal{V}_n(\mathbf{x}, \mathbf{x}) \cdot \mathcal{V}_n(\mathbf{y}, \mathbf{y})}}.$$
(9)

Here,  $V_n(\mathbf{x}, \mathbf{y})$  quantifies the strength of dependence between  $\mathbf{x}$  and  $\mathbf{y}$ , with a value of zero implying statistical independence. This quantity is computed based on the following formulation:

$$V_n^2(\mathbf{x}, \mathbf{y}) = \frac{1}{n^2} \sum_{i=1}^n \sum_{j=1}^n A_{ij} B_{ij},$$
(10)

where  $A_{ij}$  and  $B_{ij}$  are double-centered distance matrices derived from  $\mathbf{x}$  and  $\mathbf{y}$ , respectively. Then double-centered using the following formula:

$$A_{ij} = \|x_i - x_j\| - \frac{1}{n} \sum_{j'=1}^n \|x_i - x_{j'}\| - \frac{1}{n} \sum_{i'=1}^n \|x_{i'} - x_j\| + \frac{1}{n^2} \sum_{i'=1}^n \sum_{j'=1}^n \|x_{i'} - x_{j'}\|,$$
 (11)

where  $\|\cdot\|$  denotes the Euclidean norm. The same procedure applies to matrix B to obtain the centered version  $B_{ij}$ . Finally, the normalized BDC value lies within the interval [0,1], where 1 indicates perfect dependence and 0 indicates independence. Importantly, the BDC measure is strictly zero if and only if the variables are independent in the population. Therefore, it serves as a robust and comprehensive dependency metric, particularly valuable for analyzing complex, nonlinear relationships in multivariate time series.

After computing the Brownian Distance Covariance (BDC) matrix, we apply the K-means clustering algorithm on the rows of the BDC matrix to construct a *pre-assignment matrix*. Each row corresponds to a variable's dependency pattern across all other variables. Let  $\mathcal{R} \in [0,1]^{C \times C}$  denote the BDC correlation matrix among C variables. We treat each row  $\mathcal{R}_{i:} \in \mathbb{R}^{C}$  as a feature vector representing variable i, and perform K-means clustering [65] to partition the d variables into G clusters:

$$\pi = KMeans(\mathcal{R}, G), \tag{12}$$

where  $\pi \in \{1,\ldots,G\}^C$  is the cluster assignment vector. Based on these assignments, we construct a pre-assignment matrix  $P \in \{0,1\}^{C \times G}$ , where each row indicates the cluster membership of the corresponding variable using one-hot encoding. This pre-assignment matrix serves as an initial grouping prior for subsequent model components, such as channel interaction modules or hierarchical aggregation mechanisms.

# **B** Datasets

#### **B.1 TDBRAIN Dataset**

The TDBrain dataset, referenced in [66], is a large-scale EEG time series dataset containing recordings from 1,274 subjects using 33 channels. Each subject participated in two trials: one with eyes open and another with eyes closed. The dataset includes a total of 60 diagnostic labels, allowing for multi-label classification as each subject may be associated with multiple conditions. In this paper, we utilize a subset of the dataset comprising 25 subjects diagnosed with Parkinson's disease and 25 healthy controls, all under the eyes-closed condition. Each eyes-closed trial is segmented into non-overlapping 1-second windows, each containing 256 time points. Segments shorter than 1 second are discarded. This preprocessing results in a total of 6,240 samples. Each sample is tagged with a subject ID to indicate its origin.

#### **B.2** PTB-XL Dataset

The PTB-XL dataset [67] is a large-scale public ECG time series dataset collected from 18,869 subjects, each with 12-channel recordings and annotated with one or more of five labels, including four heart disease categories and one healthy control. Since each subject may have multiple trials, we remove subjects whose diagnoses vary across trials to ensure label consistency, resulting in 17,596 subjects retained. Each trial is a 10-second ECG segment, available in both 100 Hz and 500 Hz sampling rates. In our study, we use the 500 Hz version, downsampled to 250 Hz and normalized using a standard scaler. We then segment each trial into non-overlapping 1-second samples (250 time steps per sample), discarding any segment shorter than 1 second. This preprocessing yields a total of 191,400 samples. For model training, we adopt a subject-independent split, allocating 60%, 20% and 20% of subjects (and their corresponding samples) to the training, validation, and test sets, respectively.

#### **B.3** FLAAP Dataset

The FLAAP dataset [68] is a human activity recognition (HAR) dataset collected using smartphone-based inertial sensors, specifically accelerometers and gyroscopes placed at the waist of subjects. It records ten distinct daily activities performed by eight subjects, with data continuously captured between February 1st and May 31st, 2022, at a sampling rate of 100 Hz. Unlike many existing HAR datasets that focus primarily on activity classification, FLAAP emphasizes discovering associated patterns within activities, aiming to better reflect the structure of Activities of Daily Living (ADL). Each activity is segmented into fixed-length windows, producing a total of 13,123 samples with 6 sensor channels and 100 time steps per sample. In our experiments, the dataset is divided into 60% for training, 20% for validation, and 20% for testing. The dataset serves as a valuable benchmark for studying representation learning, pre-processing effects, domain transfer, and activity association mining in multivariate time series.

#### **B.4** UCI-HAR Dataset

The UCI-HAR dataset [69] is a widely used benchmark for human activity recognition (HAR), collected using smartphone-based inertial sensors. It contains recordings from 30 subjects performing six different daily activities (walking, walking upstairs, walking downstairs, sitting, standing, and lying) while carrying a smartphone equipped with a tri-axial accelerometer and gyroscope. Data were collected at a sampling rate of 50 Hz and then preprocessed by applying noise filters and segmenting the continuous signal into fixed-length windows of 2.56 seconds (128 time steps) with a 50% overlap. Each segment is labeled with the corresponding activity. In our study, we use the processed version with 9 selected channels and 128 timestamps per sample, resulting in a total of 10,299 labeled samples. The dataset is split into training and test sets based on a certain ratio.

#### **B.5** UEA Classification Dataset

The UEA dataset [47] is a comprehensive collection of multivariate time series samples spanning a wide range of application domains, primarily designed for classification tasks. It includes diverse recognition scenarios such as facial, gesture, and action recognition, as well as audio classification.

Beyond these, it serves practical purposes in areas like industrial monitoring, health surveillance, and medical diagnostics, with particular attention to cardiac data analysis. Typically, the dataset is structured into 10 distinct classes. Table 6 provides detailed classification statistics, highlighting the dataset's versatility and broad applicability across multiple domains.

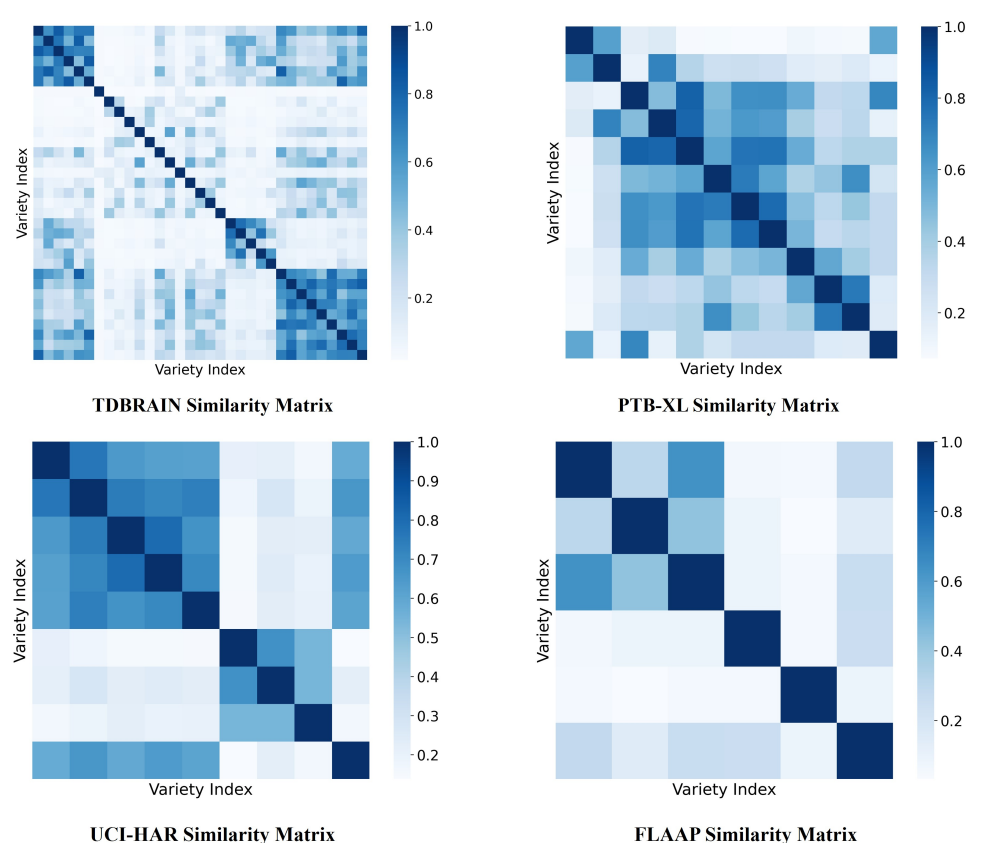
Table 6: Datasets and mapping details of UEA dataset.

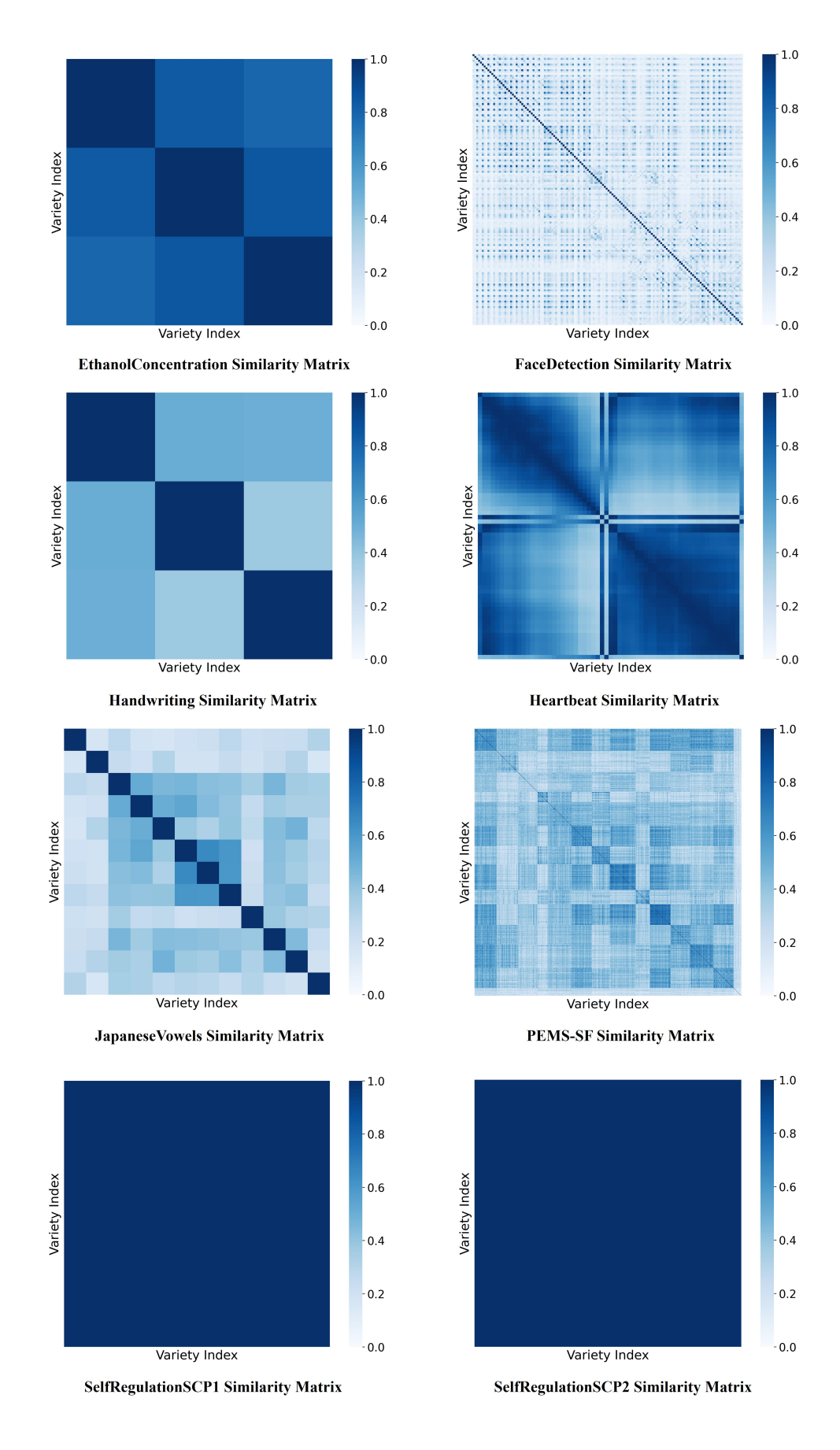
Dataset	Sample Numbers (train, test)	Variable Number	Series Length
EthanolConcentration	(261, 263)	3	1751
FaceDetection	(5890, 3524)	144	62
Handwriting	(150, 850)	3	152
Heartbeat	(204, 205)	61	405
JapaneseVowels	(270, 370)	12	29
PEMS - SF	(267, 173)	963	144
SelfRegulationSCP1	(268, 293)	6	896
SelfRegulationSCP2	(200, 180)	7	1152
SpokenArabicDigits	(6599, 2199)	13	93
UWaveGestureLibrary	(120, 320)	3	315

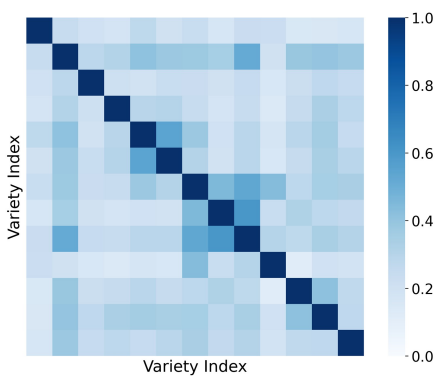
# **B.6** Datasets BDC Similarity Visualization

Figure 7 displays the similarity matrices computed using Brownian Distance Covariance (BDC) across different datasets. The x-axis and y-axis represent the variable (channel) indices.

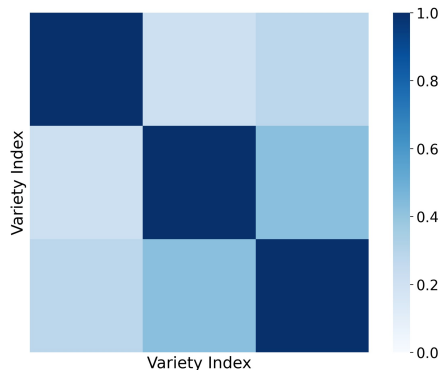
 $Figure\ 7:\ BDC\ Similarity\ Visualization\ of\ Main\ and\ UEA\ Datasets.$ 











# C Experiments Details

# **C.1** Main Datasets Implement Details

Implementation Details. All methods are implemented within a unified framework to ensure fair comparison. Specifically, we re-implement each approach using a consistent training strategy. We compare our model against a variety of state-of-the-art time series models, including six Transformer-based models, one MLP-based model, and three CNN-based models as baselines. For baseline implementations, we adopt the official code and follow the recommended best configurations. The learning rate is fixed at 0.0001, and the Adam [70] optimizer is employed for all experiments. The batch sizes are set according to the dataset: {32, 256, 32, 32} for TDBrain, PTB-XL, UCI-HAR, and FLAAP, respectively. In the data preprocessing stage, we adopt the processing pipeline from Wang[49] to ensure consistency and comparability across datasets. All models are trained for 100 epochs using five different random seeds (41 to 45), and we report the average results along with the standard deviations. To prevent overfitting, we adopt an early stopping strategy based on the F1 score on the validation set. All experiments are conducted using four NVIDIA RTX 4090 GPUs (24GB memory) with the PyTorch framework [71].

SwinGroupNet (Our Method). We perform clustering on multivariate time series based on the similarity matrix derived from BDC, generating an initial assignment matrix (see Appendix A for details). Different similarity thresholds result in different numbers of groups. We then apply Gumbel-Softmax sampling to obtain a differentiable assignment matrix, followed by independent embedding for each group. In our proposed  $Multi-Swin\ Periodic\ Window$ , multi-scale feature extraction is conducted on the input, and information from different layers is fused to produce the final output. The learning rate is set to 0.001, and an early stopping strategy is adopted. The experimental configurations on the main datasets, including the number of variable groups, the regularization parameter  $\beta$ , embedding dimension, model depth, number of kernels in depthwise convolution, period window size, and channel expansion ratio, are summarized in Table 7.

Table 7: Experiment configuration of SGN.

Dataset	# Groups	#β	# Embedding Dim	# Layers	# Kernels	# Period Window	#Channel Ratio
TDBRAIN	4	0.1	32	5	7	26	2
PTB-XL	4	0.1	64	5	7	25	2
UCI-HAR	6	0.1	64	4	7	32	2
FLAAP	5	0.1	64	2	7	50	2

#### C.2 Baselines Details

To evaluate the effectiveness of our proposed method, we selected a set of strong baseline models that cover a wide range of architectural paradigms. Specifically, for the main benchmark datasets, we include convolution-based models such as MICN [17], ModernTCN [19], and TimesNet [18]; Transformer-based models including iTransformer [24], Reformer [48], FedFormer [14], Crossformer

[25], PatchTST [22], and MedFormer [49]; and MLP-based models like DLinear [15]. These models have demonstrated strong capabilities in temporal modeling and provide a solid foundation for comparative analysis. To further validate our method, we also conducted experiments on the UEA datasets by including additional baselines such as CNN-based models (TVNet [20], TimeMixer++ [56], Rocket [52]), RNN-based models (LSTNet [50], LSSL [53]), and MLP-based models (LightTS [50], MTS-Mixer [55]).

#### C.3 Full result of UEA Datasets

Implementation Details. Our method is trained using the cross-entropy loss, with classification accuracy (%) adopted as the evaluation metric. The model is initialized with a learning rate of  $10^{-2}$ , and an early stopping strategy is applied to prevent overfitting. The symbol "\*" in Transformer-based models indicates the specific model name (e.g., \*former may refer to Informer, Crossformer, etc.). Detailed results are presented in Table 8. As shown in the table, MLP-based models exhibit relatively poor performance. In contrast, CNN-based models demonstrate superior results by effectively extracting local features and incorporating various strategies to capture global patterns.

Table 8: Performance comparison of various models on different datasets with accuracy metrics for classification.

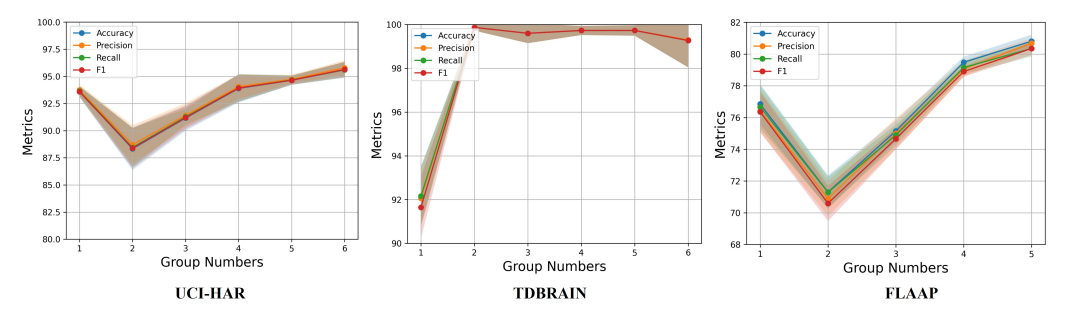
Datasets / Models	RNN-b	ased			Convolution-b	ased			MLP-ba	sed		Transfo	rmer-ba	sed		SGN
	LSTNet	LSSL	Rocket	TimesNet	ModernTCN	TVnet	Timemixer++	DLinear	LightTS	MTS-Mixer	In.	PatchTST	Cross.	Flow.	FED.	(Ours)
	2018	2022	2020	2023	2023	2025	2025	2024	2022	2023	2023	2022	2023	2022	2022	
EthanolConcentration	39.9	31.1	45.2	35.7	36.3	35.6	39.9	36.2	29.7	33.8	31.6	32.8	38.0	33.8	31.2	44.5
FaceDetection	65.7	66.7	64.7	66.0	68.0	71.2	71.8	68.0	67.5	70.2	67.0	68.7	66.1	67.6	66.0	70.3
Handwriting	25.8	24.6	58.8	32.1	27.0	32.7	26.5	26.1	27.1	33.8	32.8	29.8	30.1	33.8	28.0	50.4
Heartbeat	77.1	72.2	75.6	75.4	77.1	78.1	79.1	76.1	73.6	76.6	80.5	76.2	77.6	77.6	73.7	77.1
JapaneseVowels	98.1	98.4	96.2	98.4	98.2	98.9	97.9	96.2	96.2	94.3	98.9	97.9	99.1	98.9	98.4	98.9
PEMS-SF	86.7	86.1	75.1	89.6	89.0	91.1	91.0	88.7	87.3	90.1	81.5	89.2	90.2	86.0	80.9	88.4
SelfRegulationSCP1	84.0	90.8	90.8	91.8	91.4	93.7	93.1	90.7	92.0	95.2	90.1	92.1	92.5	92.5	88.7	93.9
SelfRegulationSCP2	52.8	52.2	53.3	54.7	56.3	60.5	65.6	50.5	51.1	55.6	53.3	56.1	56.0	56.1	54.4	60.6
SpokenArabicDigits	100.0	100.0	71.2	99.0	99.1	99.4	99.8	81.4	100.0	99.5	100.0	99.1	99.6	98.8	100	99.7
UWaveGestureLibrary	87.8	85.9	94.4	88.3	86.7	86.6	88.2	82.1	80.3	82.3	85.6	85.8	85.6	86.6	85.3	92.2
Average Accuracy	71.8	70.9	72.5	73.6	74.2	74.6	<u>75.3</u>	67.5	70.4	70.9	72.1	72.5	73.2	73.0	70.7	77.6

# **D** Hyperparamter Sensitivity

In this section, we conduct a sensitivity analysis on four key hyperparameters in the SGNet model to evaluate its robustness. Specifically, we investigate the effects of (1) the number of variable groups, (2) the number of convolution kernels, (3) the selection of periodic window sizes, and (4) the embedding dimension within each group. We present a detailed evaluation of how these hyperparameters impact model performance. The corresponding experimental results are summarized below.

**Group Numbers of Varieties.** Figure 8 presents the ablation study on variable grouping. According to the number of variables in each dataset, we partition them into {1, 2, 3, 4, 5, 6} groups. Here, a group number of 1 indicates that no grouping strategy is applied and all variables are treated jointly. We observe that as the number of groups increases, performance metrics such as accuracy initially decrease and then gradually improve. Notably, the TDBRAIN dataset exhibits a significant performance gain when variable grouping is employed, highlighting the effectiveness of our method in capturing complex inter-variable relationships.

Figure 8: Analysis of hyperparameter sensitivity concerning the group numbers on main datasets.



Embedding Dimensions and Number of kernels. Table 9 and Table 10 present the performance of our model under different embedding dimensions  $D_m \in \{16, 32, 64, 128, 256\}$  and convolution kernel sizes  $n_k \in \{3, 5, 7, 9, 11\}$ , respectively. Note that the effective receptive field of each convolutional layer is  $2n_k + 1$ . We evaluate these configurations on the main datasets.

As shown in Table 9, the TDBRAIN dataset exhibits minimal sensitivity to changes in embedding dimension, with accuracy consistently remaining above 99%. In contrast, for the other three datasets, accuracy gradually improves as the embedding dimension increases from 16 to 64. However, further increasing the dimension beyond 64 leads to a noticeable performance drop, particularly from 128 to 256. Therefore, considering both performance and computational efficiency, embedding dimensions of 32 or 64 are identified as optimal choices. And the Table 10 shows that as the number of convolution kernels increases, leading to a larger effective receptive field, the classification accuracy improves gradually. This indicates that the model is capable of extracting temporal features effectively even with smaller kernels, demonstrating its strong robustness and reduced reliance on extensive kernel coverage.

Table 9: Analysis of hyperparameter sensitivity concerning the dataembedding on main datasets.

Dataset	TDBra	ain	PTB-Z	XL	FLAA	AΡ	UCI-HAR		
Metric	Accuracy F1		Accuracy F1		Accuracy	F1	Accuracy F1		
$D_{m} = 16$ $D_{m} = 32$ $D_{m} = 64$ $D_{m} = 128$ $D_{m} = 256$	99.75 99.90 99.56 99.46 99.54	99.75 99.90 99.56 99.46 99.54	73.58 73.65 73.80 73.56 73.54	62.56 62.92 63.43 62.67 62.43	78.28 79.64 80.81 79.66 78.34	77.87 79.25 80.35 79.40 77.98	94.96 94.62 95.62 93.52 87.86	94.53 94.67 95.64 93.56 88.06	

Table 10: Analysis of hyperparameter sensitivity concerning the kernel numbers on main datasets.

Dataset	TDBra	ain	PTB-2	XL	FLAA	AΡ	UCI-HAR		
Metric	Accuracy	F1	Accuracy	F1	Accuracy	F1	Accuracy	F1	
	99.84 99.86 99.90 99.76 99.39	99.84 99.86 99.90 99.76 99.39	73.08 73.57 73.80 73.35 73.49	62.44 62.51 63.43 62.51 62.73	80.05 80.31 80.81 80.58 80.29	79.45 79.83 80.35 80.25 79.86	94.10 94.64 95.62 95.38 94.38	94.08 94.69 95.64 95.42 94.45	

**Periodic Window Sizes.** To evaluate the effectiveness of periodic window selection, we analyze the frequency-domain representations of each main dataset and select the top-5 frequencies with the highest amplitudes (excluding the full sequence length) as candidate periods. The corresponding periodic windows for each dataset are as follows: TDBRAIN (26, 128, 29, 32), FLAAP (50, 34, 25, 20), UCI-HAR (64, 32, 26, 19), and PTB-XL (84, 125, 63, 36). We then compare the model performance under these different periodic settings. As shown in Table 11, the model achieves slightly better performance under the first two period values, though the differences across configurations remain relatively small. This demonstrates the robustness of our model and validates the effectiveness of the proposed periodic mechanism for extracting multi-scale temporal information.

Table 11: Analysis of hyperparameter sensitivity concerning periodic window sizes on main datasets.

Dataset	TDBr	ain	PTB-2	ΚL	FLAA	AΡ	UCI-HAR		
Metric	Accuracy	F1	Accuracy	F1	Accuracy	F1	Accuracy	F1	
$\begin{array}{c} periodic\_window = No.1\\ periodic\_window = No.2\\ periodic\_window = No.3\\ periodic\_window = No.4\\ \end{array}$	99.69 99.58	99.90 99.69 99.58 99.79	73.34 73.56 72.91 73.09	62.54 63.65 61.59 62.48	80.81 79.08 79.24 77.45	80.35 78.66 78.77 76.94	93.88 95.62 93.95 94.50	93.95 95.64 93.97 94.49	

# E Efficiency Analysis

We conduct a comprehensive comparison between SGN and several representative models, including Reformer [48], Crossformer [25], FEDformer [14], iTransformer [24], PatchTST [22], MICN [17], ModernTCN [19], and TimesNet [18], from the perspectives of classification performance, training speed, and memory usage. As illustrated in Figure 9, SGN achieves a well-balanced trade-off between accuracy, training time, and memory consumption on the TDBRAIN and FLAAP datasets. These results highlight the efficiency and effectiveness of our proposed method in handling multivariate time series data under resource-constrained settings.

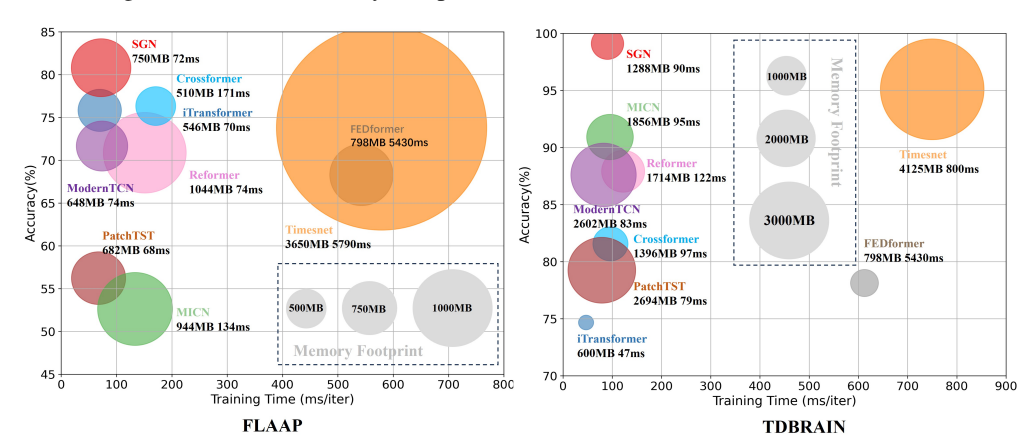


Figure 9: Model efficiency comparison under TDBRAIN and FLAAP Datesets.

#### F Additional Visualization Results

In Figure 10, we visualize the temporal correlations across different layers of the model on various datasets. It is evident that in the lower layers, temporal dependencies are mostly confined to nearby timestamps. However, with the integration of the PWSM module, which progressively merges low-level features from short-period windows into high-level representations of long-period windows, the temporal correlations in the upper layers extend across the entire window. This demonstrates the effectiveness of our multi-level periodic fusion mechanism in capturing comprehensive global temporal patterns.

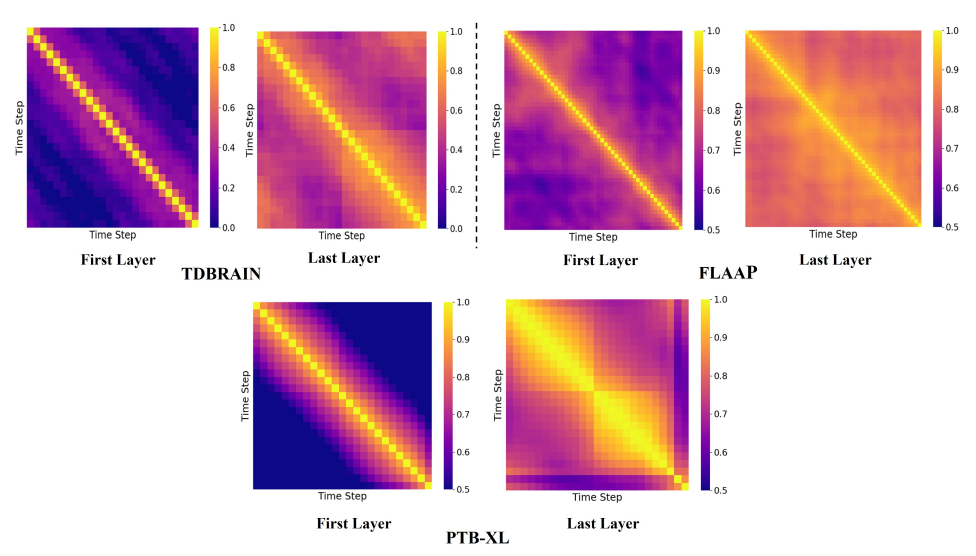


Figure 10: The temporal correlation on TDBRAIN, FLAAP and PTB-XL Datasets.

# **G** Discussion

In this paper, we propose the SGN architecture, which introduces a novel perspective for modeling variable relationships by transforming them into intra-group and inter-group interactions through variable grouping. Additionally, we leverage the periodic nature of time series to perform hierarchical and multi-scale temporal feature extraction. Our method achieves state-of-the-art performance across multiple datasets from various domains, demonstrating its generalizability and effectiveness. Despite its strong empirical results and contributions to time series modeling, SGN still has certain limitations and leaves room for further exploration.

**Limitation.** While SGN demonstrates strong performance improvements and achieves outstanding results on several datasets, its applicability to other time series tasks such as forecasting and imputation remains to be further explored. Moreover, the use of intrinsic similarity to generate the assignment matrix introduces additional computational overhead. This preprocessing step, although beneficial for modeling accuracy, may hinder deployment in real-time scenarios, and thus requires further optimization and acceleration.

**Future Work.** Future research can gradually extend SGN to other domains, such as industrial monitoring and healthcare, where multivariate time series play a crucial role. In addition, exploring alternative strategies for generating the assignment matrix, potentially guided by domain knowledge, could improve the flexibility and interpretability of variable grouping. Furthermore, enhancing the design of periodic windows, including the integration of multiple window candidates or adaptive selection mechanisms, may further boost the model's effectiveness and generalization across diverse datasets.

**Broader Impacts.** The proposed SGN model holds promising potential for positive societal impact. By enhancing the accuracy and efficiency of multivariate time series classification, SGN can benefit a wide range of critical applications. For instance, in the healthcare domain, it can help detect diseases early by analyzing patient ECG signals, leading to timely interventions and improved outcomes. In meteorology, SGN can assist in making informed decisions based on complex environmental data, ultimately contributing to risk reduction and public safety. These capabilities demonstrate the model's value in supporting well-being and societal resilience across multiple sectors.